Sensor and Simulation Notes

Note 241

July 1977

A Study of the Leaky Modes in a Finite-Width Parallel-Plate Waveguide

A. M. Rushdi
R. Menendez
R. Mittra

University of Illinois
Urbana, Illinois 61801

Abstract

This report contains the result of an investigation of the higher-order TE_z and TM_z leaky modes in a finite-width, parallel-plate waveguide. The reflection coefficient at the side openings of the guide is derived under the approximation that the interaction between the two openings is negligible. The transverse resonance condition is applied to derive the characteristic equation for the leaky modes in the open waveguide structure. Special emphasis is given to the TE_{z0} modes, which deominate the other leaky modes when the plate width is large.

CONTENTS

ILLUSTRATIONS

SECTION I

INTRODUCTION

Consider an open waveguide formed by two infinitely long, perfectly conducting, parallel plates of finite width (fig. 1). The width of each plate is denoted by w and the distance separating the plates by 2h. A coordinate system is introduced such that the z-axis coincides with the axis of the waveguide and the xy-plane is the transverse plane of the waveguide with the x-axis parallel to the plates. For later convenience, the origin of coordinates is chosen to coincide with one plate edge. A time convention [$\exp(-i\omega t)$] is assumed.

The guiding structure of figure 1 is an open structure since it does not possess walls completely impermeable to radiation and, therefore, power flow and stored energy are not confined to the inside of the guiding structure. The electromagnetic field is excited in this structure by a wave which is incident from the interior and propagates along its longitudinal (z) direction. As this wave propagates along the guide, a portion of the energy leaks out continuously through the side openings. Thus, a complete description of the electromagnetic field in the guide requires a superposition of the transverse electromagnetic (TEM) mode, higher-order transverse electric (TE) and transverse magnetic (TM) leaky modes and, finally, a continuous spectrum. This structure supports a TEM mode at all frequencies. For low frequencies the TEM mode is dominant; however, at higher frequencies for which the free space wavelength is of the same order as the cross-sectional dimensions of the guide, the TEM mode alone may not be the dominant part of the field.

The properties of the TEM mode on the guiding structure of figure 1 have been investigated using conformal mapping techniques (ref. 1 through 4). The goal of this effort was to obtain the

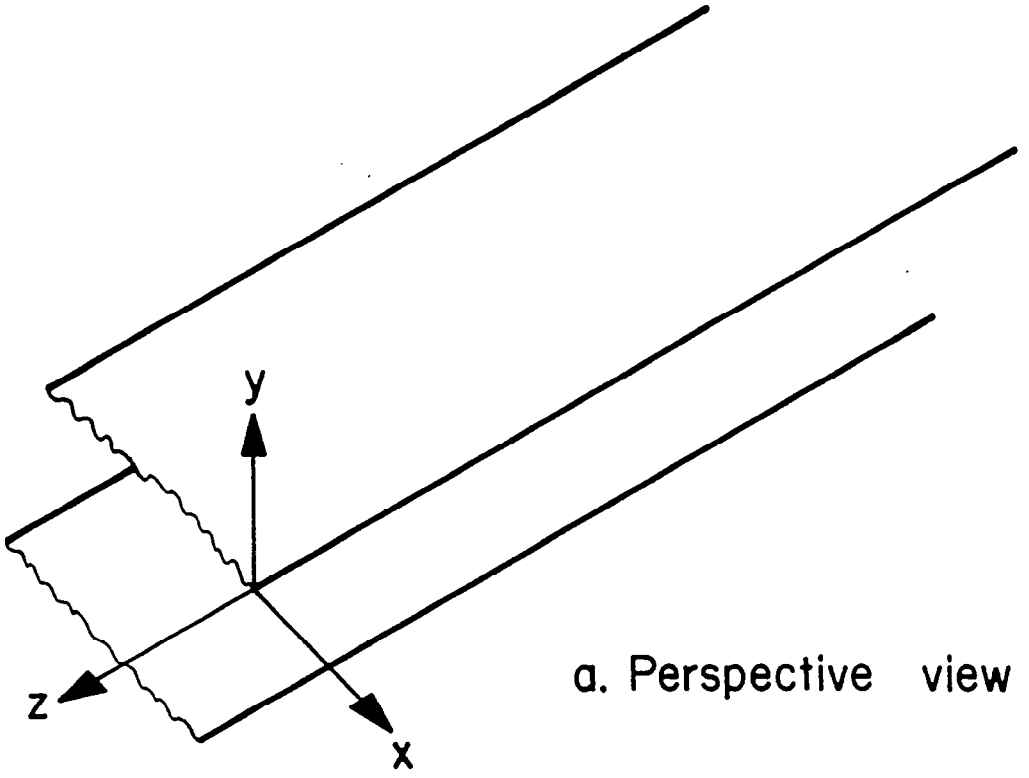

a. Perspective view

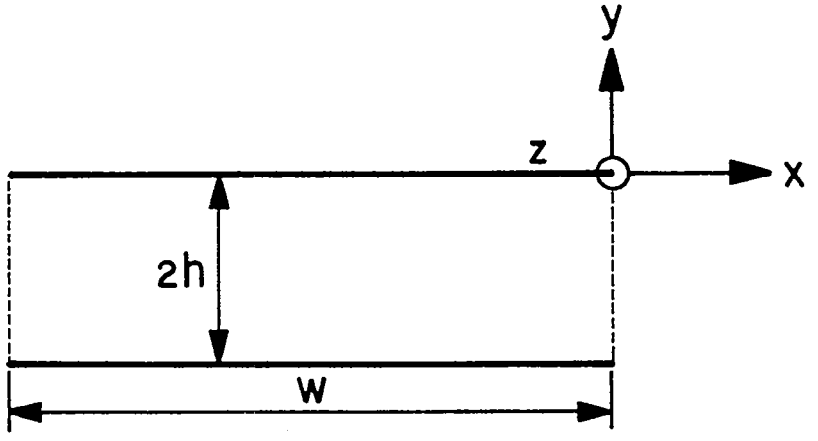

b. Transverse section

Figure 1.
Two Perfectly Conducting, Finite-Width Parallel Plates.

wave numbers and the associated field distributions for higher-order TE and TM leaky modes with the smallest axial attenuation, since it is these modes that are expected to contribute significantly to the total field. As is well known, the leaky mode expansion is an approximation to the exact continuous spectrum representation that is associated with open-region problems of the type investigated in this report.

The results obtained herein are expected to be useful in designing parallel-plate simulators for EMP studies.

SECTION II

FIELD REPRESENTATION IN TERMS OF LEAKY MODES

In contrast to open waveguides, a closed guiding structure possesses a finite cross section bounded by walls that are impermeable to radiation. Solutions to the time-harmonic source-free Maxwell's equations in such closed regions are called modes or eigenmodes. These modes are characterized by an axial field variation of the form $\exp[i(k_z z - \omega t)]$.* These modes individually satisfy all of the boundary conditions on the waveguide walls. Furthermore, the modes in conventional lossless waveguides either propagate without attenuation (k_z real) or decay exponentially without any phase variation (k_z purely imaginary). These modes are also square integrable over the cross section of the waveguide (because they have finite energy), and they possess certain orthogonality and completeness properties which make it possible to represent an arbitrary field distribution in terms of a superposition of these modes.

In contrast, the field representation in an open structure typically includes a discrete spectrum of leaky modes (ref. 5 to 7). In common with the conventional modes the leaky modes do satisfy the source-free field equations and the boundary conditions on the surface of the waveguide. However, these modes may grow without bounds at large distances away from the structure and, consequently, are not square integrable over the infinite cross section of the open waveguide. In general, these leaky modes are not members of a complete orthogonal set, and must be supplemented by a continuous spectrum if a complete representation of the field is desired.

---

*Throughout this report, ω is assumed to be real, whereas k_z can be complex.

In the guiding structure of figure 1, the axial propagation constant k_z of a leaky mode is given by

$$k_z = \beta_z + i\alpha_z \qquad \beta_z > 0 \qquad \alpha_z > 0 \tag{1}$$

which implies that the leaky modes decay as $z \to +\infty$. As a consequence (Appendix A), these modes grow exponentially in the x-direction. In fact, k_x, the propagation constant in the x-direction, belongs to the improper Riemann sheet, i.e., the sheet in which the radiation condition is violated.

In spite of the fact that the leaky modes are not proper solutions of Maxwell's equations in the entire space and do not in general form a complete set of orthogonal functions, they can nevertheless be employed to obtain convergent representations of a dominant portion of the source-excited field in certain regions in space (ref. 5 and 7) as, for example, in the region between the two parallel plates in Figure 1.

SECTION III

NATURAL DECOMPOSITION OF THE FIELD

The electromagnetic field on the uniform waveguide considered can be uniquely decomposed into two parts, one with a zero axial magnetic field (TM_z field, E-waves) and the other with zero axial electric field (TE_z field, H-waves). These two sets of fields are uncoupled. This fact is implicit in the derivations given in (ref. 8), and will be proved in section VII.

In addition, the electromagnetic field inside the guide may be symmetric or antisymmetric in the direction perpendicular to the plates, i.e., with respect to the plane $y = -h$. Hence, the field can be decomposed into two sets that are even or odd in y. Those two sets of modes are also decoupled. This fact is demonstrated in section VI.

So far the field is decomposed into four independent parts: even TE_z, odd TE_z, even TM_z and odd TM_z modes. These parts will be referred to as the four basic mode types.

A third field decomposition will be encountered when solving the modal equation of section IX. This will be according to the symmetry or antisymmetry of the field in the transverse direction parallel to the plates, i.e., x-direction. These three decompositions combine to yield eight different independent cases.

SECTION IV

THE SOLUTION OF AN AUXILIARY TWO-DIMENSIONAL PROBLEM

Mittra and Lee (ref. 8) have considered the two-dimensional problem of an electromagnetic wave incident from the inside of a semi-infinite, parallel-plate waveguide (fig. 2). They used the Jones' version of the Wiener-Hopf technique to obtain the expression for the reflected field in the waveguide. They decomposed the fields in the guide into TM and TE fields with respect to x. Since the fields have no z-variation, the nonzero field components of the TM_x fields are (H_z, E_x, E_y) and, consequently, these fields may also be considered as TE_z. Likewise, the TE_x fields (E_z, H_x, H_y) are also TM_z.

Consider a TE_z (TM_x) incident field

$$H_z = \psi_m = \cos\left(\frac{m\pi}{2h}\, y\right) e^{ik_{xm}x} \qquad m = 0,1,2,3,\ldots \tag{2}$$

where

$$k_{xm} = \left[k^2 - \left(\frac{m\pi}{2h}\right)^2\right]^{1/2} \tag{3}$$

and $k = \omega\sqrt{\mu_0\varepsilon_0}$ is the free space wavenumber. The reflected field is also TE_z (TM_x). For even m it is given by

$$\psi = S_{0m}\, e^{-ikx} + \sum_{\substack{n=2 \\ n \text{ even}}}^{\infty} S_{nm} \cos\left(\frac{n\pi}{2h}\, y\right) e^{-ik_{xn}x} \tag{4}$$

where

$$S_{0m} = -G_+(k_{xm})/G_-(k) \tag{5}$$

and

$$S_{nm} = -\frac{(k_{xn} + k)(k_{xm} + k)}{(k_{xn} + k_{xm})\, k_{xn}}\, G_+(k_{xm})G_+(k_{xm}) \tag{6}$$

for $n \neq 0$

Equations (5) and (6) can be combined into a single formula

$$S_{nm} = -\frac{(k_{xn} + k)(k_{xm} + k)}{(k_{xn} + k_{xm})\, k_{xn} \varepsilon_{0n}} G_+(k_{xn}) G_+(k_{xm}) \tag{7}$$

$\varepsilon_{0n} = 1 + \delta_{0n}$, where δ_{0n} is the Kronecker delta

$$\delta_{0n} = \begin{cases} 1 & \text{for } n = 0 \\ 0 & \text{for } n \neq 0 \end{cases} \tag{8}$$

The G_+ function in equation (7) is the plus function (ref. 8) obtained by the Wiener-Hopf factorization of the function

$$G(\eta) = G_+(\eta) G_-(\eta) = e^{-\gamma h} \frac{\sinh \gamma h}{\gamma h} \tag{9}$$

where

$$\gamma = \begin{cases} (\eta^2 - k^2)^{1/2} & \text{for } \eta > k \\ -i(k^2 - \eta^2)^{1/2} & \text{for } \eta < k \end{cases} \tag{10}$$

For odd m, the reflected field is given by

$$\psi = \sum_{\substack{n=1 \\ n \text{ odd}}}^{\infty} S_{nm} \cos\left(\frac{n\pi}{2h} y\right) e^{-ik_{xn}x} \tag{11}$$

where

$$S_{nm} = -i \frac{(k_{xn} + k)^{1/2} (k_{xm} + k)^{1/2}}{h(k_{xn} + k_{xm})\, k_{xn}} L_+(k_{xn}) L_+(k_{xm}) \tag{12}$$

The L_+ function is the plus function obtained by the Wiener-Hopf factorization of the function

$$L(\eta) = L_+(\eta) L_-(\eta) = e^{-\gamma h} \cosh \gamma h \tag{13}$$

Explicit expressions for $G_+(\eta)$ and $L_+(\eta)$ are given in appendix B.

Now, consider a TM_z (TE_x) incident field, given by

$$E_{zm} = \phi_m = \sin\left(\frac{m\pi}{2h}\, y\right) e^{ik_{xm}x} \qquad m = 1,2,3,\ldots \tag{14}$$

The reflected field is also TM_z (TE_x). For even m it is given by

$$\phi = \sum_{\substack{n=2 \\ n \text{ even}}}^{\infty} S_{nm} \sin\left(\frac{n\pi}{2h}\, y\right) e^{-ik_{xn}x} \tag{15}$$

where

$$S_{nm} = -mn\left(\frac{\pi}{2h}\right)^2 \frac{G_+(k_{xn})G_+(k_{xm})}{k_{xn}(k_{xn} + k_{xm})} \tag{16}$$

For odd m, the reflected field is given by

$$\phi = \sum_{\substack{n=1 \\ n \text{ odd}}}^{\infty} S_{nm} \sin\left(\frac{n\pi}{2h}\, y\right) e^{-ik_{xn}x} \tag{17}$$

where

$$S_{nm} = \frac{-imn\left(\frac{\pi}{2h}\right)^2 L_+(k_{xn})\, L_+(k_{xm})}{hk_{xn}(k_{xn} + k_{xm})(k_{xn} + k)^{1/2}(k_{xm} + k)^{1/2}} \tag{18}$$

Observe that S_{nm} as defined by equations (7), (12), (16), and (18) for even TE_z, odd TE_z , even TM_z and odd TM_z modes, respectively, can be interpreted as the reflection coefficient from the m^{th} mode to the n^{th} mode (fig. 2) evaluated at the edge (x = 0, y = 0).

The coupling effects are neglected between the two openings at x = 0 and x = -w of the open waveguide of figure 1. This means that the reflection coefficient for this configuration also will be given by S_{nm}.

SECTION V

THE THREE-DIMENSIONAL PROBLEM

In the previous section a two-dimensional problem was considered, where the incident wave propagates in the transverse plane. Now, consider the same problem with an obliquely incident wave with an axial variation of $\exp[ik_z z]$. Since the structure of figure 1 is invariant under translation in the z-direction, the reflected wave has the same z-variation as the incident one. In view of this, the original three-dimensional problem can be reduced to an equivalent two-dimensional one. In fact, it turns out that the solution to the three-dimensional problem can be deduced from that of the two-dimensional problem discussed in the previous section.

Each of the incident $(\bar{E}^i,\bar{H}^i)$, reflected $(\bar{E}^r,\bar{H}^r)$ or total $(\bar{E}^t,\bar{H}^t)$ fields can be expressed as

$$\begin{Bmatrix} \bar{E}(x,y,z) \\ \bar{H}(x,y,z) \end{Bmatrix} = \begin{Bmatrix} \bar{e}(x,y) \\ \bar{h}(x,y) \end{Bmatrix} e^{ik_z z} \tag{19}$$

where $\bar{E}$ and $\bar{H}$ satisfy the homogeneous vector Helmholtz equation

$$(\nabla^2 + k^2) \begin{Bmatrix} \bar{E}(x,y,z) \\ \bar{H}(x,y,z) \end{Bmatrix} = \begin{Bmatrix} \bar{0} \\ \bar{0} \end{Bmatrix} \tag{20}$$

which, by virtue of equation (19), can be reduced to

$$\left(\nabla_t^2 + k_t^2\right) \begin{Bmatrix} \bar{e}(x,y) \\ \bar{h}(x,y) \end{Bmatrix} = \begin{Bmatrix} \bar{0} \\ \bar{0} \end{Bmatrix} \tag{21}$$

where

$$\nabla_t^2 = \nabla^2 - \frac{\partial^2}{\partial z^2} = \frac{\partial^2}{\partial x^2} + \frac{\partial^2}{\partial y^2} \tag{22}$$

and

$$k_t^2 = k^2 - k_z^2 \tag{23}$$

Thus, the conditions on the reflected field $(\bar{E}^r, \bar{H}^r)$ are that it satisfy:

a. the two-dimensional Helmholtz equation (21);

b. the boundary conditions on the two conducting plates, i.e., at $y = 0, -2h$ and $-w \leq x \leq 0$.

$$\bar{e}^t \times \hat{y} = \bar{0} \quad \text{and} \quad \frac{\partial}{\partial y} [\bar{h} \cdot \hat{y}] = 0$$

or equivalently,

$$\bar{e}^r \times \hat{y} = -\bar{e}^i \times \hat{y} \tag{24}$$

and

$$\frac{\partial}{\partial y} [\bar{h}^r \cdot \hat{y}] = - \frac{\partial}{\partial y} [\bar{h}^i \cdot \hat{y}] \tag{25}$$

c. the edge condition as $(x^2 + y^2) \to 0$.

In view of these conditions, it is clear that $(\bar{E}^r, \bar{H}^r)$ is precisely the solution of the two-dimensional problem discussed in the previous section, provided that a multiplicative constant of $\exp[ik_z z]$ is inserted and k is replaced by k_t.

Thus, the reflection coefficient in the three-dimensional problem is given by the expressions of section IV once k is replaced by k_t.

SECTION VI

RAY INTERPRETATION

If the two side openings of the parallel-plate guiding structure of figure 1 are closed with conducting plates, one gets a conventional rectangular waveguide. The field inside this guide is composed of TE_z and TM_z modes. Some insight into the behavior of these modes is obtained by decomposing them into plane TEM waves. The field of TE_{0n} (or TM_{0n}) modes can be decomposed into the sum of two plane TEM waves propagating along zigzag paths between the guide walls (fig. 3). Equivalently, this field can be pictured as produced by a plane wave reflecting back and forth between the guide walls.

Actually, this field can be expressed as

$$U = \left(e^{ik_{yn}y} + \tau\, e^{-ik_{yn}y}\right) e^{ik_{zn}z} \tag{26}$$

where

$$U = \begin{Bmatrix} H_z \\ E_z \end{Bmatrix}, \quad \tau = \begin{Bmatrix} +1 \\ -1 \end{Bmatrix} \text{ for } \begin{Bmatrix} TE_z \text{ modes} \\ TM_z \text{ modes} \end{Bmatrix} \tag{27}$$

and

$$k^2 = k_{yn}^2 + k_{zn}^2 \tag{28}$$

τ represents the self-reflection coefficient of the $0n^{th}$ mode. For perfectly conducting plates there is no coupling upon reflection between different modes. The boundary conditions at the conducting plates $y = 0$ and $y = -2h$ require that k_{yn} take on discrete values $\frac{n\pi}{2h}$ where n is an integer.

The two terms of equation (26) represent plane waves because they have plane wavefronts, i.e., plane surfaces of constant phase. The curves everywhere

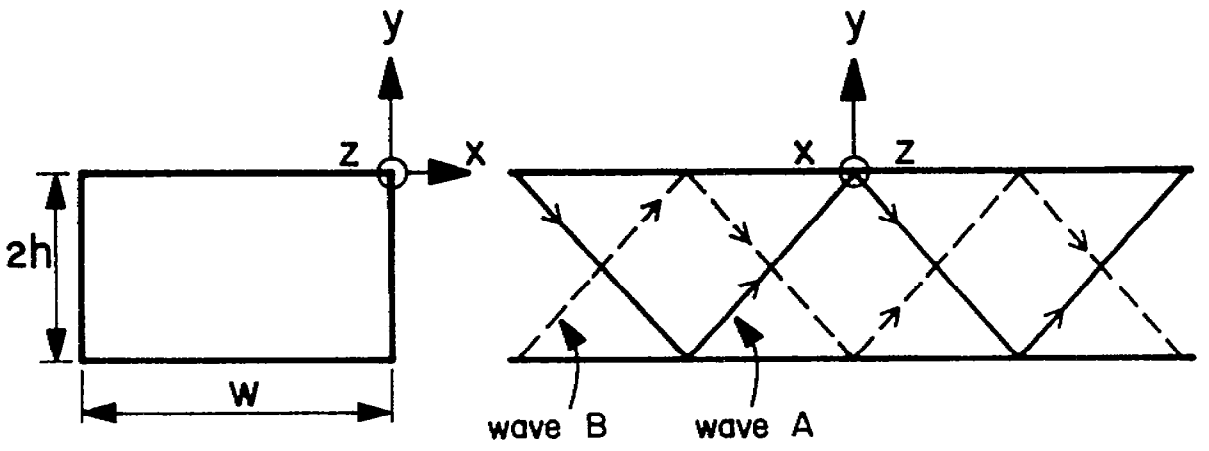

Figure 3.

Decomposition of TE_{0n} Modes into Two Plane Waves in a Conventional Rectangular Waveguide.

orthogonal to these wavefronts (called rays) are straight lines along the direction of the propagation vectors

$$\bar{k}^{\mp} = \mp k_{yn}\hat{y} + k_{zn}\hat{z}$$

$$= \mp k \sin \phi_n \, \hat{y} + k \cos \phi_n \, \hat{z} \qquad (29)$$

where the angle ϕ_n is as defined in figure 3.

The decomposition of TE_{0n} modes into two plane waves may be extended into TE_{mn} and TM_{mn} modes also. When m and n are both different from zero, four plane waves result (ref. 9).

Now, if a similar decomposition is performed on the modes inside the open waveguide of figure 1, then one gets the four plane waves

$$U = \exp[i(\mp k_x x \mp k_y y + k_z z)] \qquad (30)$$

where

$$k^2 = k_x^2 + k_y^2 + k_z^2 \qquad (31)$$

The propagation vectors

$$\bar{k} = \mp k_x \hat{x} \mp k_y \hat{y} + k_z \hat{z} \qquad (32)$$

are now complex, and equation (30) is said to represent inhomogeneous plane waves or complex rays. These waves can be considered to reflect back and forth between the conducting plates at y = 0 and y = -2h with reflection coefficients τ as given by equation (27). The boundary conditions at the conducting plates require that k_y be real and is given by

$$k_y = k_{ym} = \frac{m\pi}{2h} \qquad m = \text{integer} \qquad (33)$$

The wave having $k_y = k_{ym}$ (which we called the m^{th} mode) will have the corresponding k_x denoted by k_{xm}.

The four-wave decomposition of equation (30) can be rearranged for the m^{th} mode as

$$
\begin{aligned}
U_m^{++} &= \exp\left\{i\left[k_{xm}x + \left(\frac{m\pi}{2h}\right) y + k_z z\right]\right\} \\
U_m^{+-} &= \exp\left\{i\left[k_{xm}x - \left(\frac{m\pi}{2h}\right) y + k_z z\right]\right\} \\
U_m^{-+} &= \exp\left\{i\left[-k_{xm}x + \left(\frac{m\pi}{2h}\right) y + k_z z\right]\right\} \\
U_m^{--} &= \exp\left\{i\left[-k_{xm}x - \left(\frac{m\pi}{2h}\right) y + k_z z\right]\right\}
\end{aligned}
\tag{34}
$$

which can be replaced by a two-wave decomposition

$$
\begin{aligned}
U_m^{+} &= U_m^{++} + \tau U_m^{+-} \\
&= 2\left\{\begin{matrix} \cos\left(\frac{m\pi}{2h}\, y\right) \\ i \sin\left(\frac{m\pi}{2h}\, y\right) \end{matrix}\right\} e^{ik_{xm}x}\, e^{ik_z z}
\end{aligned}
\tag{35}
$$

$$
\begin{aligned}
U_m^{-} &= U_m^{-+} + \tau U_m^{--} \\
&= 2\left\{\begin{matrix} \cos\left(\frac{m\pi}{2h}\, y\right) \\ i \sin\left(\frac{m\pi}{2h}\, y\right) \end{matrix}\right\} e^{-ik_{xm}}\, e^{ik_z z}
\end{aligned}
\tag{36}
$$

The two plane waves equations (35) and (36) reflect back and forth between the openings x = 0 and x = -w. Since energy leakage takes place at these openings, we now expect the self-reflection coefficients to have magnitudes less than unity. Moreover, coupling takes place between different modes upon reflection.

As before, S_{nm} is defined as the reflection coefficient from the plane wave of the m^{th} mode to that of the n^{th} mode at one opening of an open-ended waveguide (fig. 2).

Lee [ref. 10] has derived an expression for S_{nm} by considering the following ray picture. Let the ray M be incident on the edge (x = 0, y = 0) of the parallel-plate waveguide of figure 2. Let N be a ray scattered from the edge and let the ray I be an image to the ray M with respect to y = 0. The rays M and N correspond to appropriate plane wave components of the m^{th} and n^{th} modes referred to above. Specifically, M corresponds to U_m^{++} and N corresponds to U_n^{--}.

For the two-dimensional problems, i.e., no z-variation, the transverse propagation vectors $\bar{k}_{tm} = k_{xm}\hat{x} + k_{ym}\hat{y}$ and $\bar{k}'_{tn} = -k_{xn}\hat{x} - k_{yn}\hat{y}$ are real and represent the directions of the rays. In this case we define the angles θ_m, θ_n, ψ^i, and ψ^r as shown in figure 4. All of these angles are measured in a clockwise sense; thus, according to the usual convention, they will be negative.

$$\psi^i = -\pi + (\theta_n - \theta_m) \tag{37}$$

$$\psi^r = \pi + (\theta_n + \theta_m) \tag{38}$$

For rays incident from or reflected to the inside of the guide, we have

$$-\pi < \theta_i < -\frac{\pi}{2} \qquad i = m,n \tag{39}$$

These angles are complex for the three-dimensional problem. In this case we define θ_m and θ_n by

$$\left\{ \begin{array}{l} \cos\theta_i = -\dfrac{k_{xi}}{k_t} \\ \\ \sin\theta_i = -\dfrac{k_{yi}}{k_t} \end{array} \right\} \qquad i = m,n \tag{40}$$

and we define ψ^i and ψ^r in terms of θ_m and θ_n via equations (37) and (38).

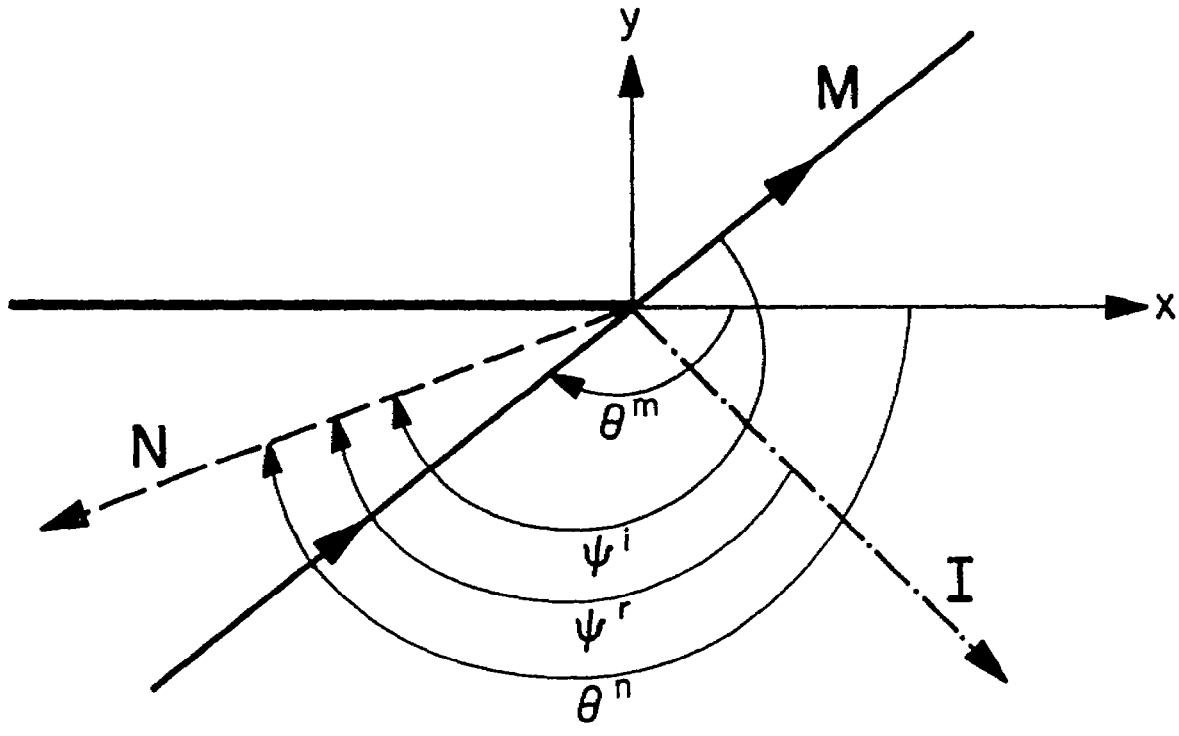

Figure 4.

A Real Ray Picture of the Two-Dimensional Problem.

The problem of figure 2 is now replaced by two equivalent problems for the determination of modes that are even or odd in y (fig. 5a and 5b, respectively). The validity of this replacement (ref. 8 and 10) is a proof of the decoupling of modes even in y from those odd in y.

The edge diffraction coefficient $\bar{D}(\theta_n,\theta_m)$ from the ray M to the ray N is given by

$$\bar{D}(\theta_n,\theta_m) = D(\theta_n,\theta_m)\ f(\theta_n)\ f(\theta_m) \tag{41}$$

The factor $D(\theta_n,\theta_m)$ is known as the diffraction coefficient for a half plane and is given by

$$D(\theta_n,\theta_m) = \frac{i}{2}\left[\frac{1}{\sin\left(\frac{\psi^i}{2}\right)} + \frac{\tau}{\sin\left(\frac{\psi^r}{2}\right)}\right] \tag{42}$$

This can be written as

$$D(\theta_n,\theta_m) = \begin{cases} \dfrac{2i\sin\left(\frac{\theta_n}{2}\right)\sin\left(\frac{\theta_m}{2}\right)}{\cos\theta_n + \cos\theta_m} & \text{for } TE_z \text{ modes} \\ & (\tau = 1) \\ \dfrac{-2i\cos\left(\frac{\theta_n}{2}\right)\cos\left(\frac{\theta_m}{2}\right)}{\cos\theta_n + \cos\theta_m} & \text{for } TM_z \text{ modes} \\ & (\tau = -1) \end{cases} \tag{43}$$

or equivalently

$$D(\theta_n,\theta_m) = \begin{cases} \dfrac{-i(k_t + k_{xn})^{1/2}(k_t + k_{xm})^{1/2}}{(k_{xn} + k_{xm})} & \text{for } TE_z \text{ modes} \\ \dfrac{i(k_t - k_{xn})^{1/2}(k_t - k_{xm})^{1/2}}{(k_{xn} + k_{xm})} & \text{for } TM_z \text{ modes} \end{cases} \tag{44}$$

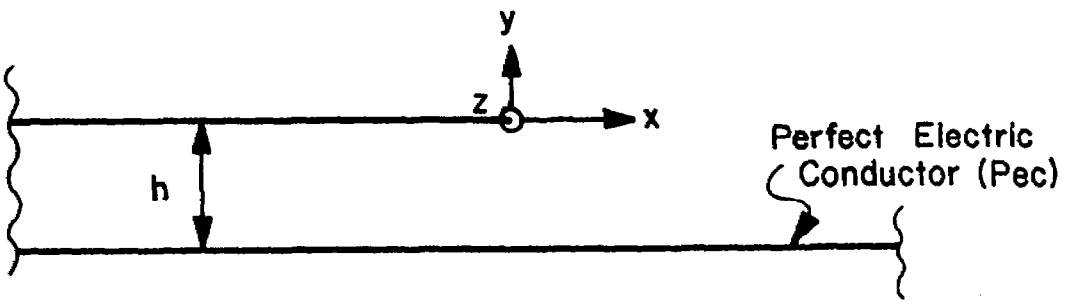

Figure 5a.

A Problem Equivalent to that in figure 2 for Modes Even in y.

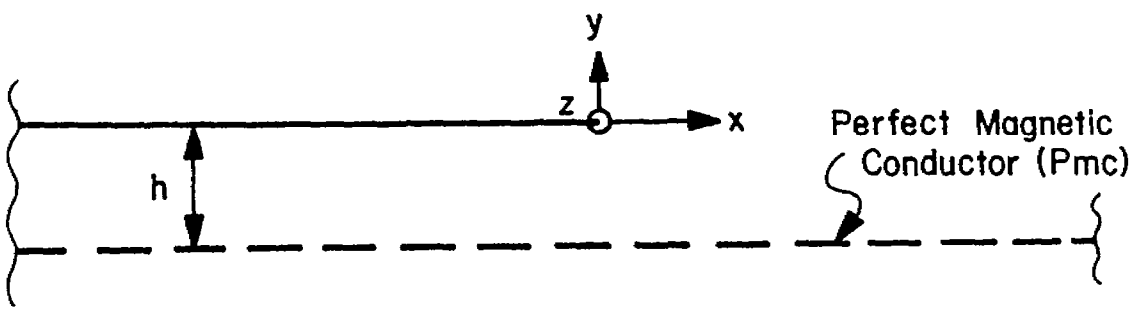

Figure 5b.

A Problem Equivalent to that in figure 2 for Modes Odd in y.

In equation (41), $D(\theta_n,\theta_m)$ is modified with $f(\theta_n)\ f(\theta_m)$ in order to account for the interaction between the edge at (x = 0, y = 0) and the lower plate at y = -h (fig. 5a) along the shadow boundary at x = 0.

$$f(\theta_i) = \begin{cases} [2h(k_t + k_{xi})]^{1/2}\ e^{-i\frac{\pi}{4}}\ G_+(k_{xi}) & \text{even } i \\ \sqrt{2}\ L_+(k_{xi}) & \text{odd } i \end{cases} \tag{45}$$

where the G_+ and L_+ functions are those previously mentioned in section IV.

Now S_{nm} is obtained by multiplying $\bar{D}(\theta_n,\theta_m)$ by τC_n

$$S_{nm} = \tau C_n D(\theta_n,\theta_m)\ f(\theta_n)\ f(\theta_m) \tag{46}$$

where τ is as defined in equation (27) and C_n is the ray-to-mode conversion factor, given by

$$C_n = -[2\epsilon_{0n}k_t h \cos\theta_n]^{-1} = [2\epsilon_{0n}k_{xn}h]^{-1} \tag{47}$$

It is evident from equation (46) that $S_{nm} \neq S_{mn}$ for $n \neq m$. With the aid of equations (44)-(47) we can deduce the expressions for S_{nm} for the four basic mode types. Those expressions are the same as those given by equations (7), (12), (16) and (18) when k is replaced by k_t.

SECTION VII

DECOUPLING OF TE_z AND TM_z MODES

Each of the incident, reflected or total fields referred to in section V can be decomposed in terms of TE_z and TM_z modes, derivable from two scalar potentials h_z and e_z, respectively.

TE_z modes

$$\bar{E}_z = \bar{0}$$

$$\bar{H}_z = h_z e^{+ik_z z} \hat{a}_z$$

$$\bar{H}_t = + \frac{ik_z}{k_t^2} \nabla_t h_z e^{+ik_z z} = \frac{1}{k_t^2} \left[\nabla_t \frac{\partial}{\partial z} H_z \right]$$

$$\bar{E}_t = +Z\hat{a}_z \times \bar{H}_t \qquad (48)$$

where $Z = - \frac{\omega\mu}{k_z}$ is the wave impedance of a given TE_z mode.

TM_z modes

$$\bar{H}_z = \bar{0}$$

$$\bar{E}_z = e_z e^{+ik_z z} \hat{a}_z$$

$$\bar{E}_t = + \frac{ik_z}{k_t^2} \nabla_t e_z e^{+ik_z z} = \frac{1}{k_t^2} \left[\nabla_t \frac{\partial}{\partial z} E_z \right]$$

$$\bar{H}_t = -Y\hat{a}_z \times \bar{E}_t \qquad (49)$$

where $Y = - \frac{\omega\epsilon}{k_z}$ is the wave admittance of a certain TM_z mode.

If we introduce the quantities

$$\bar{U}(\bar{r}) = \begin{Bmatrix} \bar{H} \\ \bar{E} \end{Bmatrix} = \begin{Bmatrix} \bar{H}_t + \bar{H}_z \\ \bar{E}_t + \bar{E}_z \end{Bmatrix} \qquad u(x,y) = \begin{Bmatrix} h_z \\ e_z \end{Bmatrix} \text{ for } \begin{Bmatrix} TE_z \\ TM_z \end{Bmatrix} \text{ fields} \qquad (50)$$

then from equations (48) and (49),

$$\bar{U}(\bar{r}) = \left[\frac{ik_z}{k_t^2} \nabla_t u(x,y) + u(x,y) \right] e^{ik_z z} \tag{51}$$

If the incident ray M referred to in section VI is TE_z or TM_z, then it can be expressed in terms of equation (51) with

$$u(x,y) = e^{i(k_{xm}x + k_{ym}y)} \tag{52}$$

which means that this ray M is represented by the field vector

$$\bar{U} = \bar{U}_m^{++} = \bar{V}_m^{++} e^{i\bar{k}_m \cdot \bar{r}} \tag{53}$$

where

$$\bar{k}_m = k_{xm}\hat{x} + k_{ym}\hat{y} + k_z\hat{z} \tag{54}$$

and

$$\bar{V}_m^{++} = -\frac{k_{xm}k_z}{k_t^2}\hat{x} - \frac{k_{ym}k_z}{k_t^2}\hat{y} + \hat{z} \tag{55}$$

Similarly, if the diffracted ray N referred to in section VI is TE_z or TM_z, then it can be represented in terms of equation (51) with

$$u(x,y) = e^{-i(k_{xn}x + k_{yn}y)} \tag{56}$$

which means that this ray N is represented by the field vector

$$\bar{U} = \bar{U}_n^{--} = \bar{V}_n^{--} e^{i\bar{k}'_n \cdot \bar{r}} \tag{57}$$

where

$$\bar{k}'_n = -k_{xn}\hat{x} - k_{yn}\hat{y} + k_z\hat{z} \tag{58}$$

and

$$\bar{V}_n^{--} = \frac{k_{xn} k_z}{k_t^2} \hat{x} + \frac{k_{yn} k_z}{k_t^2} \hat{y} + \hat{z} \tag{59}$$

We observe that the plane electromagnetic waves equations (53) and (57) satisfy the condition

$$\bar{V}_m^{++} \cdot \bar{k}_m = 0 \tag{60}$$

$$\bar{V}_n^{--} \cdot \bar{k}_n' = 0 \tag{61}$$

Let a diffracted field vector due to the incident TE_z (or TM_z) field vector equation (53) be

$$\bar{W}_n^{--} = \bar{W}_n^{--} e^{i\bar{k}_n' \cdot \bar{r}} \tag{62}$$

Though the incident ray equation (53) is either TE_z or TM_z, the diffracted ray equation (62) is assumed, for the moment, to be a combination thereof. However, since equation (62) represents a plane electromagnetic wave,

$$\bar{W}_n^{--} \cdot \bar{k}_n' = 0 \tag{63}$$

Similarly, a general incident plane electromagnetic wave may be given by

$$\bar{W}_m^{++} = \bar{W}_m^{++} e^{i\bar{k}_m \cdot \bar{r}} \tag{64}$$

where

$$\bar{W}_m^{++} \cdot \bar{k}_m = 0 \tag{65}$$

Consider the decomposition of W_m^{++} into components in and normal to the edge fixed plane of incidence (EFPI) which is the plane of the diffracting edge and the wavevector $\bar{k}_m$ (fig. 6). Now introduce the

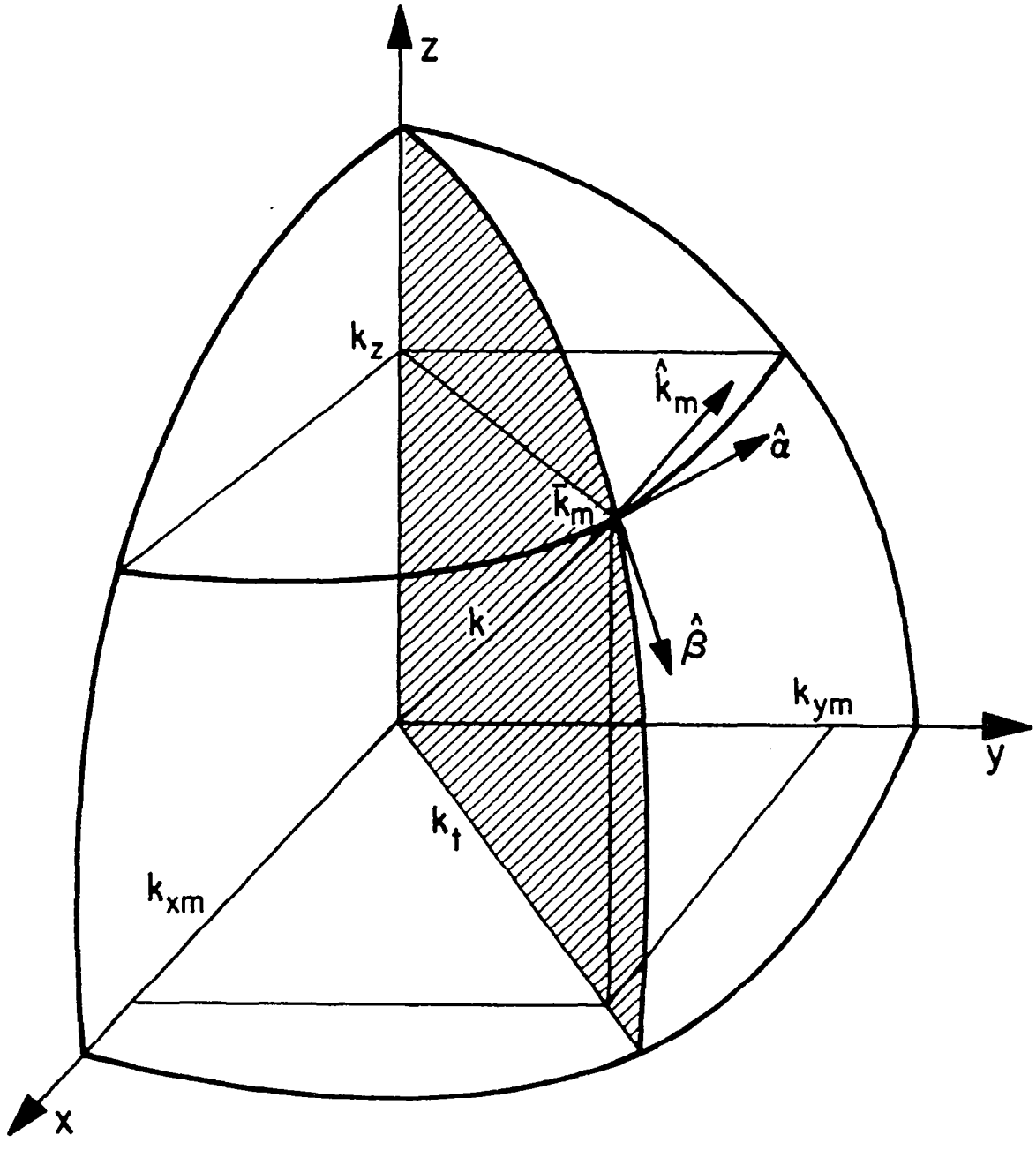

Figure 6.
Pertaining to the Coordinate Triad ($\hat{\alpha}$, $\hat{k}_m$, $\hat{\beta}$).

orthonormal triad $(\hat{\alpha},\hat{k}_m,\hat{\beta})$ such that $\hat{\alpha}$ is a unit vector normal to EFPI, $\hat{k}_m = \frac{\bar{k}_m}{|\bar{k}_m|}$ and $\hat{\beta}$ is a unit vector in EFPI normal to $\hat{k}_m$. Due to equation (65), $\bar{\bar{W}}_m^{++}$ has no $\hat{k}_m$ component, i.e.,

$$\bar{\bar{W}}_m^{++} = \tilde{W}_\alpha \hat{\alpha} + \tilde{W}_\beta \hat{\beta} \tag{66}$$

The symbol ~ indicates that the vector components are referred to the $(\hat{\alpha},\hat{k}_m,\hat{\beta})$ basis.

The relation of the orthonormal triad $(\hat{\alpha},\hat{k}_m,\hat{\beta})$ to the orthonormal triad $(\hat{x},\hat{y},\hat{z})$ is the well-known relation between a spherical coordinate system and a Cartesian system. Hence

$$\hat{\alpha} = -\frac{k_{ym}}{k_t}\hat{x} + \frac{k_{xm}}{k_t}\hat{y}$$

$$\hat{k}_m = \frac{k_{xm}}{k}\hat{x} + \frac{k_{ym}}{k}\hat{y} + \frac{k_{zm}}{k}\hat{z}$$

$$\hat{\beta} = \frac{k_{xm}k_z}{k_t k}\hat{x} + \frac{k_{ym}k_z}{k_t k}\hat{y} - \frac{k_t}{k}\hat{z} \tag{67}$$

The representation of the vector $\bar{\bar{W}}_m^{++}$ with respect to the basis $(\hat{x},\hat{y},\hat{z})$ and its representation $\tilde{\bar{\bar{W}}}_m^{++}$ with respect to the basis $(\hat{\alpha},\hat{k}_m,\hat{\beta})$ are related by the unitary transformations

$$\tilde{\bar{\bar{W}}}_m^{++} = [T_m^{++}]\,\bar{\bar{W}}_m^{++} \tag{68}$$

$$\bar{\bar{W}}_m^{++} = [T_m^{++}]^t\,\tilde{\bar{\bar{W}}}_m^{++} \tag{69}$$

where

$$\tilde{\bar{\bar{W}}}_m^{++} = [\tilde{W}_\alpha, \tilde{W}_{km}, \tilde{W}_\beta]^t \tag{70}$$

$$\bar{\bar{W}}_m^{++} = [W_x, W_y, W_z] \tag{71}$$

and

$$[T_m^{++}] = \begin{bmatrix} -\frac{k_{ym}}{k_t} & \frac{k_{xm}}{k_t} & 0 \\ \frac{k_{xm}}{k} & \frac{k_{ym}}{k} & \frac{k_z}{k} \\ \frac{k_{xm}k_z}{k_t k} & \frac{k_{ym}k_z}{k_t k} & \frac{-k_t}{k} \end{bmatrix} \tag{72}$$

$[T_m^{++}]^t$ is the transpose (and also inverse) of $[T_m^{++}]$.

Similarly, the vector $\bar{W}_n^{--}$ can have another representation $\tilde{\bar{W}}_n^{--}$ with respect to an appropriate basis $(\hat{\alpha}', \hat{k}_n', \hat{\beta}')$, with

$$\tilde{\bar{W}}_n^{--} = [T_n^{--}]\, \bar{W}_n^{--} \tag{73}$$

and

$$\bar{W}_n^{--} = [T_n^{--}]^t\, \tilde{\bar{W}}_n^{--} \tag{74}$$

where

$$[T_n^{--}](k_{xn}, k_{yn}, k_z) = [T_n^{++}](-k_{xn}, -k_{yn}, k_z) \tag{75}$$

Now, observe that substituting $\bar{V}_m^{++}$ from equation (55) in place of $\bar{W}_m^{++}$ in equation (68) yields

$$\tilde{\bar{V}}_m^{++} = -\frac{k}{k_t}\,\hat{\beta} \tag{76}$$

Equation (76) is a special case of equation (66). It indicates that $\bar{E}$ for a TM_z incident field or $\bar{H}$ for a TE_z incident field is entirely along the $\hat{\beta}$-direction. Similarly $\bar{E}$ for a TM_z diffracted field or $\bar{H}$ for a TE_z diffracted field is entirely along the $\hat{\beta}'$ direction.

The incident and diffracted rays equations (53) and (62) evaluated at $\bar{r} = \bar{0}$ are related

$$\bar{W}_n^{--} = [D_{nm}]\, \bar{V}_m^{++} \tag{77}$$

If these rays are referred to the $(\hat{\alpha},\hat{k}_m,\hat{\beta})$ and $(\hat{\alpha}',\hat{k}_n',\hat{\beta}')$ bases, respectively, then equation (77) takes the form

$$\bar{\tilde{W}}_n^{--} = [\tilde{D}_{nm}]\,\bar{\tilde{V}}_m^{++} \tag{78}$$

Lee and Deschamps [ref. 11] have shown that the dyadic $[\tilde{D}_{nm}]$ in equation (78) is diagonalized. Due to equations (63) and (76) the second diagonal element of $[\tilde{D}_{nm}]$ is irrelevant and can be set arbitrariiy to zero. Then write

$$[\tilde{D}_{nm}] = \begin{bmatrix} D_- & 0 & 0 \\ 0 & 0 & 0 \\ 0 & 0 & D_+ \end{bmatrix} \tag{79}$$

where D_+ and D_- are the so-called soft and hard diffraction coefficients.

Making use of equations (74), (78) and (68), we obtain

$$\bar{W}_n^{--} = [T_n^{--}][\tilde{D}_{nm}][T_m^{++}]\,\bar{V}_m^{++} \tag{80}$$

Substituting for the quantities in the right-hand side from equations (75), (79), (72), and (55), get

$$\bar{W}_n^{--} = D_+\left[\frac{k_{xn}k_z}{k_t^2}\,\hat{x} + \frac{k_{yn}k_z}{k_t^2}\,\hat{y} + \hat{z}\right] \tag{81}$$

which, by virtue of equation (59), becomes

$$\bar{W}_n^{--} = D_+\bar{V}_n^{--} \tag{82}$$

Equation (82) simplifies the problem significantly, so a dyadic operation to express the diffracted field in terms of the incident field is no longer needed. Rahter, consider the incident field to be

TE_z (TM_z) derivable from a scalar potential h_z (e_z) having a unit amplitude when evaluated at $\bar{r} = \bar{0}$. The diffracted field will also be TE_z (TM_z) derivable from a scalar potential $h_z(e_z)$ having an amplitude equal to D_+ when evaluated at $\bar{r} = \bar{0}$. This procedure has already been utilized in section VI.

Basically, the dyadic operation in equation (79) rotates the $\bar{k}$ $\bar{E}$ $\bar{H}$ triad about the plate edge [ref. 11]. Obviously for a TE_z (TM_z) field where the E_z (H_z) component is zero, a rotation of the field about the edge (z-direction) cannot introduce an E_z (H_z) component. This means that a TE_z (TM_z) incident ray gives rise only to a diffracted TE_z (TM_z) ray, which again proves the decoupling of TE_z and TM_z modes.

SECTION VIII

TRANSVERSE RESONANCE CONDITION

Consider the geometry in figure 7 and let a wave be incident between the plates from the left to the right. No generality is lost by restricting this wave to any of the four basic types of modes considered in section III. Let the scalar potential of the m^{th} mode of this wave be

$$u_m = a_m \begin{Bmatrix} \cos\left(\frac{m\pi}{2h} y\right) \\ \sin\left(\frac{m\pi}{2h} y\right) \end{Bmatrix} e^{ik_{xm}x} \tag{83}$$

where

$$u_m = \begin{Bmatrix} h_{zm} \\ e_{zm} \end{Bmatrix} \text{ for } \begin{Bmatrix} TE_z \\ TM_z \end{Bmatrix} \text{ modes} \tag{84}$$

and

$$m = \begin{cases} 0,2,4\ldots \text{ for the even } TE_z \text{ set} \\ \quad 2,4\ldots \text{ for the even } TM_z \text{ set} \\ 1,3,5\ldots \text{ for the odd sets} \end{cases} \tag{85}$$

This incident wave will give rise to a reflected wave (belonging to the same set) whose n^{th} mode is given by

$$u_n = \left(\sum_m S_{nm} a_m\right) \begin{Bmatrix} \cos\left(\frac{n\pi}{2h} y\right) \\ \sin\left(\frac{n\pi}{2h} y\right) \end{Bmatrix} e^{-ik_{xn}x} \tag{86}$$

which, upon the change of coordinates $x = -(x' + w)$ [fig. 7], becomes

$$u_n = b_n \begin{Bmatrix} \cos\left(\frac{n\pi}{2h} y\right) \\ \sin\left(\frac{n\pi}{2h} y\right) \end{Bmatrix} e^{ik_{xn}x'} \tag{87}$$

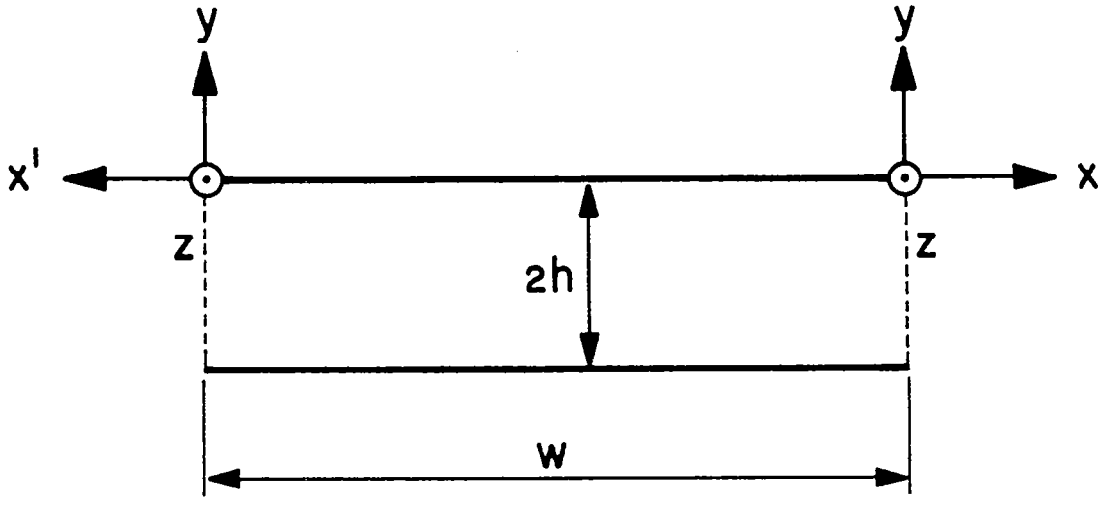

Figure 7.

Auxiliary Coordinates for the Structure in figure 1, Used to Illustrate the Derivation of the Transverse Resonance Condition.

where

$$b_n = \left(\sum_m S_{nm} a_m \right) e^{ik_{xn} w} \tag{88}$$

Now, this wave reflected at the right opening $x = 0$ will be incident on the left opening $x = -w$ ($x' = 0$), giving rise to a reflected wave whose ℓ^{th} mode is

$$v_\ell = \left(\sum_n S_{\ell n} b_n \right) \begin{Bmatrix} \cos \left(\frac{\ell \pi}{2h} y \right) \\ \sin \left(\frac{\ell \pi}{2h} y \right) \end{Bmatrix} e^{-ik_{xn} x'} \tag{89}$$

The transverse resonance condition can now be written as

$$v_\ell \left(x' = -\frac{w}{2} \right) = u_m \left(x = -\frac{w}{2} \right) \delta_{\ell m} \quad , \quad \text{for all } m \tag{90}$$

where $\delta_{\ell m}$ is the Kronecker delta defined by equation (8). Hence

$$\sum_n \sum_m S_{\ell n} S_{nm} e^{i(k_{x\ell} + 2k_{xn} + k_{xm}) \frac{w}{2}} a_m = a_m \delta_{\ell m} \quad \text{for all } m \tag{91}$$

If we let

$$R_{nm} = S_{nm} e^{i(k_{xn} + k_{xm}) \frac{w}{2}} \tag{92}$$

then, by interchanging the order of summation in equation (91), one gets

$$\sum_m \left(\sum_n R_{\ell n} R_{nm} \right) a_m = \delta_{\ell m} a_m \quad \text{for all } m \tag{93}$$

R_{nm} can be interpreted as the reflection coefficient from the m^{th} mode to the n^{th} mode, evaluated at the center plane $x = x' = -\frac{w}{2}$.

The equation (93) can be combined in a compact matrix form

$$[R][R]\,\bar{A} = [I]\,\bar{A} \tag{94}$$

where $\bar{A}$ is the modal amplitude vector (evaluated at the opening x = 0) with elements a_m at the m^{th} row, [R] is a square matrix with elements R_{nm} at the n^{th} row and m^{th} column, and [I] is the identity matrix.

Theoretically the dimensions of both $\bar{A}$ and [R] are infinite; however, they are truncated to some finite dimension N.

If equation (94) is written as

$$\{[R][R] - [I]\}\,\bar{A} = \bar{0} \tag{95}$$

then $\bar{A}$ has a nontrivial solution only if the determinant of the matrix between the curly brackets is zero, i.e.,

$$\mathrm{Det}\{[R][R] - [I]\} = 0 \tag{96}$$

Making use of the identity

$$\mathrm{Det}\{[Q_1][Q_2]\} = \mathrm{Det}[Q_1]\ \mathrm{Det}[Q_2] \tag{97}$$

one can reduce equation (96) into the following two equations

$$\mathrm{Det}\{[R] - [I]\} = 0 \tag{98}$$

or

$$\mathrm{Det}\{[R] + [I]\} = 0 \tag{99}$$

which correspond, respectively, to the vector eigenvalue problems

$$\{[R] - [I]\}\,\bar{A} = \bar{0} \tag{100}$$

and

$$\{[R] + [I]\}\,\bar{A} = \bar{0} \tag{101}$$

These, when combined together, are equivalent to the original eigenvalue equation (95).

Equations (98) and (99) are the modal equations for modes whose axial field components $u = \begin{Bmatrix} h_z \\ e_z \end{Bmatrix}$ are respectively symmetrical and anti-symmetrical with respect to the center plane $x = -\frac{w}{2}$.

SECTION IX

SOLUTION OF THE MODAL EQUATION

For a specific mode type and physical dimensions, [R] is a function only of the transverse wavenumber k_t. This means that k_t is the unknown to be determined from our modal equations (98) and (99) . This procedure is similar to the one discussed in references 8 and 14. Once k_t is known, k_z is readily obtained from the relationship $k_z = \sqrt{k^2 - k_t^2}$.

The solution of the modal equations (98) and (99) amounts to finding the complex roots k_z of complex transcendental functions. This type of problem has been discussed in references 12 and 13. In [ref. 12] Muller discusses an iterative method that has been programmed under the name ZANLYT for the DEC system 10 and CDC CYBER 175 FORTRAN VERSION 4 Compilers. The Muller method requires knowledge of the approximate root(s) of the complex function and it is unreliable for complex functions of exponential behavior. In [ref. 13] Cauchy's theorem is used to find the number and location of zeros of an analytic function in a given contour. The second was especially suitable for our purpose, since it allowed us to search for the zeros of the functions in (98) and (99) within a rectangular region of the first quadrant in the complex k_z ($= \beta_z + i\alpha_z$) plane. The rectangle was defined by

$$0 < \beta_z < k \qquad 0 < \alpha_z << k \tag{102}$$

The roots obtained by the SEARCH and HOMEIN subroutines of reference 13 were improved further by the Muller method. The absolute value of the complex function was reduced to less than 10^{-6} at the location of a root.

Let $k_{z\ell}^s$ and $k_{z\ell}^a$ be the roots of the symmetrical equation (98) and the antisymmetrical equation (99), and let the corresponding k_x be

denoted by $k^s_{xm\ell}$ and $k^a_{xm\ell}$, respectively. Here ℓ (= 0,1,2...) and m as given by equation (85) are the indices associated with the field variations in the two transverse directions x and y, respectively. An even (odd) ℓ corresponds to a mode symmetrical (antisymmetrical) in x. The modal amplitudes vectors $\bar{A}^s_\ell$ and $\bar{A}^a_\ell$ can now be obtained by solving

$$[R - I]\left(k^s_{z\ell}\right) \bar{A}^s_\ell = \bar{0} \tag{103}$$

and

$$[R + I]\left(k^a_{z\ell}\right) \bar{A}^a_\ell = \bar{0} \tag{104}$$

To be specific, let us consider the solution of equation (103). The matrix $[B] = [R - I]\ k^s_{z\ell}$ is an N × N matrix with a zero determinant. If we assume that the order of this zero is L where $1 \leq L \leq N$, then the rank of the matrix [B] is (N - L). In this case, the equation $[B]\ \bar{A} = \bar{0}$ has L nontrivial, independent solutions for $\bar{A}$. For low-order modes (low ℓ) we do not expect multiple roots, i.e., L = 1, implying that there is a unique field distribution associated with a certain $k^s_{z\ell}$. For higher ℓ, L can be greater than 1, and a multiplicity of degenerate solutions may be associated with the same $k^s_{z\ell}$.

The solutions $\bar{A}^s_\ell$ of equation (103) and $\bar{A}^a_\ell$ of equation (104) can thus be obtained numerically with minor modifications of a subroutine designed to calculate the generalized eigenvectors of a complex matrix.

SECTION X

FIELD DISTRIBUTION OF THE MODES IN THE REGION BETWEEN THE PLATES

The scalar potential u of any of the four basic mode sets is given by

$$u = \begin{cases} \sum_{\ell} \left[\bar{C}_{\ell}^{s}\right]^{t} \bar{A}_{\ell}^{s} \, e^{ik_{z\ell}^{s} z} & (105) \\ \sum_{\ell} \left[\bar{C}_{\ell}^{a}\right]^{t} \bar{A}_{\ell}^{a} \, e^{ik_{z\ell}^{a} z} & (106) \end{cases}$$

for sets symmetrical and antisymmetrical in x, respectively.

The m^{th} elements of vector matrices $\bar{C}_{\ell}^{s}$ and $\bar{C}_{\ell}^{a}$ are, respectively,

$$\frac{1}{2} \begin{Bmatrix} \cos\left(\frac{m\pi}{2h} y\right) \\ \sin\left(\frac{m\pi}{2h} y\right) \end{Bmatrix} \left[e^{ik_{xm\ell}^{s} x} + e^{-ik_{xm\ell}^{s}(x+w)} \right] \qquad (107)$$

and

$$\frac{1}{2i} \begin{Bmatrix} \cos\left(\frac{m\pi}{2h} y\right) \\ \sin\left(\frac{m\pi}{2h} y\right) \end{Bmatrix} \left[e^{ik_{xm\ell}^{a} x} - e^{-ik_{xm\ell}^{a}(x+w)} \right] \qquad (108)$$

$$\text{for} \begin{Bmatrix} TE_z \\ TM_z \end{Bmatrix} \text{modes}$$

Using equations (107) and (108), the expressions for u can be simplified to

$$u = \begin{cases} \sum_{\ell} \sum_{m} a_{m\ell}^{s} \begin{Bmatrix} \cos\left(\frac{m\pi}{2h} y\right) \\ \sin\left(\frac{m\pi}{2h} y\right) \end{Bmatrix} e^{-ik_{xm\ell}^{s} \frac{w}{2}} \cos\left[k_{xm\ell}^{s}\left(x + \frac{w}{2}\right)\right] e^{ik_{z\ell}^{s} z} & (109) \\ \sum_{\ell} \sum_{m} a_{m\ell}^{a} \begin{Bmatrix} \cos\left(\frac{m\pi}{2h} y\right) \\ \sin\left(\frac{m\pi}{2h} y\right) \end{Bmatrix} e^{-ik_{xm\ell}^{a} \frac{w}{2}} \sin\left[k_{xm\ell}^{a}\left(x + \frac{w}{2}\right)\right] e^{ik_{z\ell}^{a} z} & (110) \end{cases}$$

It is noteworthy that once the eigenvector equations (103) and (104) are solved for $\bar{A}_{\ell}^{s,a}$, the parameters $\{a_{m\ell}^{s,a} : \forall_m\}$ are not all arbitrary, for they can be given in terms of a single arbitrary constant. With this in mind, and apart from differences of notation, we can observe that equations (109) and (110) are essentially the same as equations (87) and (84) of Marin reference 14.

Now, equations (109) or (110) can be used together with equations (49) or (50) to yield the following field distribtuion of the modes in the region between the plates:

$\underline{TE_z \text{ modes}}$

$$\begin{Bmatrix} H_z^s \\ H_z^a \end{Bmatrix} = \sum_{\ell} \sum_{m} \cos\left(\frac{m\pi}{2h} y\right) \begin{Bmatrix} \cos\left[k_{xm\ell}^s \left(x + \frac{w}{2}\right)\right] \\ \sin\left[k_{xm\ell}^a \left(x + \frac{w}{2}\right)\right] \end{Bmatrix} \begin{Bmatrix} F_{m\ell}^s(z) \\ F_{m\ell}^a(z) \end{Bmatrix} \tag{111}$$

$$\begin{Bmatrix} \bar{H}_t^s \\ \bar{H}_t^a \end{Bmatrix} = i \sum_{\ell} \sum_{m} \left[\cos\left(\frac{m\pi}{2h} y\right) \begin{Bmatrix} -k_{xm\ell}^s \sin\left[k_{xm\ell}^s \left(x + \frac{w}{2}\right)\right] \\ k_{xm\ell}^a \cos\left[k_{xm\ell}^a \left(x + \frac{w}{2}\right)\right] \end{Bmatrix} \hat{x} \right.$$

$$\left. - \frac{m\pi}{2h} \sin\left(\frac{m\pi}{2h} y\right) \begin{Bmatrix} \cos\left[k_{xm\ell}^s \left(x + \frac{w}{2}\right)\right] \\ \sin\left[k_{xm\ell}^a \left(x + \frac{w}{2}\right)\right] \end{Bmatrix} \hat{y} \right] \begin{Bmatrix} F_{m\ell}^s(z) \dfrac{k_{z\ell}^s}{k_{t\ell}^{s2}} \\ F_{m\ell}^a(z) \dfrac{k_{z\ell}^a}{k_{t\ell}^{a2}} \end{Bmatrix} \tag{112}$$

$$\begin{Bmatrix} \bar{E}_t^s \\ \bar{E}_t^a \end{Bmatrix} = -i\omega\mu \sum_\ell \sum_m \left[\frac{m\pi}{2h} \sin\left(\frac{m\pi}{2h}\, y\right) \begin{Bmatrix} \cos\left[k_{xm\ell}^s \left(x + \frac{w}{2}\right)\right] \\ \sin\left[k_{xm\ell}^a \left(x + \frac{w}{2}\right)\right] \end{Bmatrix} \hat{x} \right.$$

$$\left. + \cos\left(\frac{m\pi}{2h}\, y\right) \begin{Bmatrix} -k_{xm\ell}^s \sin\left[k_{xm\ell}^s \left(x + \frac{w}{2}\right)\right] \\ k_{xm\ell}^a \cos\left[k_{xm\ell}^a \left(x + \frac{w}{2}\right)\right] \end{Bmatrix} \hat{y} \right] \begin{Bmatrix} F_{m\ell}^s(z)/k_{t\ell}^{s2} \\ F_{m\ell}^a(z)/k_{t\ell}^{a2} \end{Bmatrix} \quad (113)$$

$\underline{TM_z \text{ modes}}$

$$\begin{Bmatrix} E_z^s \\ E_z^a \end{Bmatrix} = \sum_\ell \sum_m \sin\left(\frac{m\pi}{2h}\, y\right) \begin{Bmatrix} \cos\left[k_{xm\ell}^s \left(x + \frac{w}{2}\right)\right] \\ \sin\left[k_{xm\ell}^a \left(x + \frac{w}{2}\right)\right] \end{Bmatrix} \begin{Bmatrix} F_{m\ell}^s(z) \\ F_{m\ell}^a(z) \end{Bmatrix} \quad (114)$$

$$\begin{Bmatrix} \bar{E}_t^s \\ \bar{E}_t^a \end{Bmatrix} = i \sum_\ell \sum_m \left[\sin\left(\frac{m\pi}{2h}\, y\right) \begin{Bmatrix} -k_{xm\ell}^s \sin\left[k_{xm\ell}^s \left(x + \frac{w}{2}\right)\right] \\ k_{xm\ell}^a \cos\left[k_{xm\ell}^a \left(x + \frac{w}{2}\right)\right] \end{Bmatrix} \hat{x} \right.$$

$$\left. + \frac{m\pi}{2h} \cos\left(\frac{m\pi}{2h}\, y\right) \begin{Bmatrix} \cos\left[k_{xm\ell}^s \left(x + \frac{w}{2}\right)\right] \\ \sin\left[k_{xm\ell}^a \left(x + \frac{w}{2}\right)\right] \end{Bmatrix} \hat{y} \right] \begin{Bmatrix} F_{m\ell}^s(z) k_{z\ell}^s / k_{t\ell}^{s2} \\ F_{m\ell}^a(z) k_{z\ell}^a / k_{t\ell}^{a2} \end{Bmatrix} \quad (115)$$

$$\begin{Bmatrix} \bar{H}_t^s \\ \bar{H}_t^a \end{Bmatrix} = -\omega\varepsilon \sum_\ell \sum_m \left[-\frac{m\pi}{2h} \cos\left(\frac{m\pi}{2h}\, y\right) \begin{Bmatrix} \cos\left[k_{xm\ell}^s \left(x + \frac{w}{2}\right)\right] \\ \sin\left[k_{xm\ell}^a \left(x + \frac{w}{2}\right)\right] \end{Bmatrix} \hat{x} \right.$$

$$\left. + \sin\left(\frac{m\pi}{2h}\, y\right) \begin{Bmatrix} -k_{xm\ell}^s \sin\left[k_{xm\ell}^s \left(x + \frac{w}{2}\right)\right] \\ k_{xm\ell}^a \cos\left[k_{xm\ell}^a \left(x + \frac{w}{2}\right)\right] \end{Bmatrix} \hat{y} \right] \begin{Bmatrix} F_{m\ell}^s(z)/k_{t\ell}^2 \\ F_{m\ell}^a(z)/k_{t\ell}^2 \end{Bmatrix} \quad (116)$$

where

$$\begin{Bmatrix} F^s_{m\ell}(z) \\ F^a_{m\ell}(z) \end{Bmatrix} = \begin{Bmatrix} a^s_{m\ell} \exp\left(-ik^s_{xm\ell}\frac{w}{2}\right) \exp\left(ik^s_{z\ell}z\right) \\ a^a_{m\ell} \exp\left(-ik^a_{xm\ell}\frac{w}{2}\right) \exp\left(ik^s_{z\ell}z\right) \end{Bmatrix} \tag{117}$$

In the special case of wide plates

$$\xi = \frac{h}{w} << 1 \tag{118}$$

Then, out of the higher-order leaky modes, only the TE_z modes of order $m = 0$ have a significant contribution to the total field. For these modes the field components are given by

$$\begin{Bmatrix} H^s_z \\ H^a_z \end{Bmatrix} = \sum_\ell \begin{Bmatrix} \cos\left[k_{x0\ell}\left(x + \frac{w}{2}\right)\right] \\ \sin\left[k_{x0\ell}\left(x + \frac{w}{2}\right)\right] \end{Bmatrix} \begin{Bmatrix} F^s_{0\ell}(z) \\ F^a_{0\ell}(z) \end{Bmatrix} \tag{119}$$

$$\begin{Bmatrix} H^s_x \\ H^a_x \end{Bmatrix} = i \sum_\ell \begin{Bmatrix} -\sin\left[k^s_{x0\ell}\left(x + \frac{w}{2}\right)\right] \\ \cos\left[k^a_{x0\ell}\left(x + \frac{w}{2}\right)\right] \end{Bmatrix} \begin{Bmatrix} F^s_{0\ell}(z)\,\frac{k^s_{z\ell}}{k^s_{x0\ell}} \\ F^a_{0\ell}(z)\,\frac{k^a_{z\ell}}{k^a_{x0\ell}} \end{Bmatrix} \tag{120}$$

$$\begin{Bmatrix} E^s_y \\ E^a_y \end{Bmatrix} = -i\omega\mu \sum_\ell \begin{Bmatrix} -\sin\left[k^s_{x0\ell}\left(x + \frac{w}{2}\right)\right] \\ \cos\left[k^a_{x0\ell}\left(x + \frac{w}{2}\right)\right] \end{Bmatrix} \begin{Bmatrix} F^s_{0\ell}(z)/k^s_{x0\ell} \\ F^a_{0\ell}(z)/k^a_{x0\ell} \end{Bmatrix} \tag{121}$$

where the parameters $a^s_{0\ell}$ and $a^a_{0\ell}$ in $F^s_{0\ell}(z)$ and $F^a_{0\ell}(z)$ are obtained by solving the scalar eigenvalue problem that is obtained by truncating the dimensions of $[R]$ and $\bar{A}$ (section VIII) of the even TE_z set to $N = 1$. In the following section, this problem will be considered further and an approximate solution for it will be developed which is valid for

$$|k_{x0\ell}w| >> 1 \quad \text{and} \quad |k_{x0\ell}h| << 1 \tag{122}$$

SECTION XI

APPROXIMATE MODAL SOLUTION FOR SINGLE TE_z MODES WITH m = 0

The self-reflection coefficient for the TE_{z0} modes can be written from equation (5) as

$$S_{00} = -G_+^2(k_{x0}) \tag{123}$$

Boersma (ref. 15) and Weinstein (ref. 16) found that for small $|k_{x0}h|$ they could take equal to unity all multiple factors other than $B^e(k_{x0})$ in the expression (B.1) for $G_+(k_{x0})$, so that

$$S_{00} = -\exp\left\{\frac{i2k_{x0}h}{\pi}\left[\ell n\left(\frac{2\pi}{k_{x0}h}\right) + (1 - C) + \frac{\pi i}{2}\right] + O\left(k_{x0}^2h^2\right)\right\} \tag{124}$$

where C is the Euler constant

$$C = \lim_{n\to\infty}\left[1 + \frac{1}{2} + \ldots + \frac{1}{n} - \ell n\ n\right] = 0.57716 \tag{125}$$

The transverse resonance condition for a single TE_{z0} mode can be written as a special case of equation (91) as

$$S_{00}\, e^{ik_{x0}w} = e^{i\pi\ell} \tag{126}$$

where, as before, ℓ is the index associated with the variations in the x direction.

$$\ell = \begin{cases} 0,2,4\ldots & \text{for modes symmetrical in x} \\ 1,3,5\ldots & \text{for modes antisymmetrical in x} \end{cases} \tag{127}$$

Equation (126) can be rewritten as

$$k_{x0\ell}w + \frac{2k_{x0\ell}h}{\pi}\left[\ell n\left(\frac{2\pi}{k_{x0\ell}h}\right) + (1 - C) + \frac{\pi i}{2}\right] = (\ell + 1)\,\pi + O\left(k_{x0\ell}^2 h^2\right) \quad (128)$$

If we let

$$P_{0\ell} = k_{x0\ell}w = |P_{0\ell}|\, e^{i\phi_{0\ell}} \quad (129)$$

then the solution of equation (128) is obtained as the zero for the function $f(P_{0\ell})$ defined by

$$f(P_{0\ell}) = P_{0\ell} + \frac{2}{\pi} P_{0\ell}\xi\left[\ell n\left(\frac{2\pi}{P_{0\ell}\xi}\right) + (1 - C) + \frac{\pi i}{2}\right] - (\ell + 1)\,\pi + O\left(P_{0\ell}^2\xi^2\right) \quad (130)$$

where the logarithm in equation (130) is interpreted (appendix B) as

$$\ell n\left(\frac{2\pi}{P_{0\ell}\xi}\right) = \ell n\left(\frac{2\pi}{|P_{0\ell}|\xi}\right) - i\phi_{0\ell} \quad (131)$$

A solution $P_{0\ell}$ of equation (130) is expected to be in the fourth quadrant $\left(-\frac{\pi}{2} < \phi_{0\ell} < 0\right)$. Due to the approximation in equation (124), our modal equation (130) is now not dependent on both h and w but rather on their ratio ξ. Since $\lim_{\xi \to 0} \xi \log \xi = 0$, one gets

$$P_{0\ell} \to \pi(\ell + 1) \quad \text{as } \xi \to 0 \quad (132)$$

which could have been anticipated.

Under the conditions (122), the root of (130) is obtained as

$$P_{0\ell} = \left\{1 + \frac{2}{\pi}\,\xi\left[\ell n\left(\frac{2\pi}{P_{0\ell}\xi}\right) + (1 - C) + i\,\frac{\pi}{2}\right]\right\}^{-1}(\ell + 1)\,\pi + O\left(P_{0\ell}^2\xi^2\right)$$

$$\approx \left\{1 - \frac{2}{\pi}\,\xi\left[\ell n\left(\frac{2\pi}{P_{0\ell}\xi}\right) + (1 - C) + i\,\frac{\pi}{2}\right]\right\}(\ell + 1)\,\pi + O\left(P_{0\ell}^2\xi^2\right) + O(\xi^2) \tag{133}$$

A perturbational solution for $P_{0\ell}$ is obtained if we substitute $(\ell + 1)\,\pi$ for it in the right-hand side of equation (133).

$$P_{0\ell} \approx \left(1 - \frac{2}{\pi}\,\xi\left\{\ell n\left[\frac{2}{(\ell + 1)\,\xi}\right] + (1 - C) + i\,\frac{\pi}{2}\right\}\right)(\ell + 1)\,\pi + O\left(P_{0\ell}^2\xi^2\right) + O(\xi^2) \tag{134}$$

For $\ell = 0$, the first of the conditions (122) is not quite satisfied, so P_{00} obtained by equation (134) is not very accurate.

If only the leading terms of the real and imaginary parts are retained in equation (134), then it is simplified to

$$P_{0\ell} \approx (\ell + 1)\,\pi\,[1 - i\xi] \qquad |\xi| << 1 \tag{135}$$

For the first few lower-order modes

$$\chi_\ell = \frac{(\ell + 1)\,\pi}{kw} << 1 \tag{136}$$

then the axial propagation constant k_z is given by equation (1).

$$k_{z0\ell} = k\sqrt{1 - \left(\frac{P_{0\ell}}{kw}\right)^2}$$

$$\approx k\sqrt{1 - \chi_\ell^2}\,\left(1 + i\xi\chi_\ell^2\right) \tag{137}$$

which has positive real and imaginary parts, in accordance with equation (1).

From equation (118), the transverse field distribution is given by

$$\begin{Bmatrix} H^s_{z0\ell} \\ H^a_{z0\ell} \end{Bmatrix} \sim \begin{Bmatrix} \cos k^s_{x0\ell} x_1 \\ \sin k^a_{x0\ell} x_1 \end{Bmatrix} = \begin{Bmatrix} \cos \beta^s_{x0\ell} x_1 \cosh \alpha^s_{x0\ell} x_1 - i \sin \beta^s_{x0\ell} x_1 \sinh \alpha^s_{x0\ell} x_1 \\ \sin \beta^a_{x0\ell} x_1 \cosh \alpha^a_{x0\ell} x_1 + i \cos \beta^a_{x0\ell} x_1 \sinh \alpha^a_{x0\ell} x_1 \end{Bmatrix} \tag{138}$$

where

$$x_1 = x + \frac{w}{2} \tag{139}$$

which under the conditions (122) can be simplified with the aid of (135) to

$$\mathrm{Re} \begin{Bmatrix} H^s_{z0\ell} \\ H^a_{z0\ell} \end{Bmatrix} \sim \begin{Bmatrix} \cos \beta^s_{x0\ell} x_1 \\ \sin \beta^a_{x0\ell} x_1 \end{Bmatrix} = \begin{Bmatrix} \cos (k\chi_\ell x_1) \\ \sin (k\chi_\ell x_1) \end{Bmatrix} \tag{140}$$

and

$$\mathrm{Im} \begin{Bmatrix} H^s_{z0\ell} \\ H^a_{z0\ell} \end{Bmatrix} \sim \begin{Bmatrix} -\alpha^s_{x0\ell} x_1 \sin \beta^s_{x0\ell} x_1 \\ \alpha^a_{x0\ell} x_1 \cos \beta^a_{x0\ell} x_1 \end{Bmatrix}$$

$$= \begin{Bmatrix} \xi(k\chi_\ell x_1) \sin (k\chi_\ell x_1) \\ -\xi(k\chi_\ell x_1) \cos (k\chi_\ell x_1) \end{Bmatrix} \tag{141}$$

Marin [ref. 14] has considered a similar problem under the assumptions $|k_t h| \ll 1$ and $\xi \ll 1$, which are identical to those employed in this section. After changing his notation as indicated below

$$S \to j\omega, \quad P \to -jk_t, \quad 2w \to w \tag{142}$$

his equation (82) reads

$$S_{oo}\, e^{ik_t w}\, (1+h\sqrt{\frac{2k_t}{\pi w}}\; e^{-i\frac{\pi}{4}}) = -1 \qquad (143)$$

where S_{oo} is given by the approximate formula (124) and the branch cut for the square root function is taken just above the positive real axis of the complex plane.

Equation (143) which is the characteristic equation for antisymmetrical TE_{zo} modes differs from equation (126) by the factor

$$f = 1 + h\sqrt{\frac{2\,k_t}{\pi w}}\; e^{-i\frac{\pi}{4}} \qquad (144)$$

The presence of the additional factor f was first noted in a recent work by Krichevsky and Mittra, where an explanation of its physical meaning was also given. However, under the assumption expressed in (122), which is valid for wide plates, the factor f in equation (144) becomes essentially equal to unity. Thus, the results reported here may be viewed as having negligible error.

Table 1 compares some calculated values of the complex wavenumbers of the lowest-order $TE_{zo\ell}$ modes, using the approximate equation (130), the more exact equations (98), (99), and the perturbational formula (133). Corresponding field variations are plotted in Figs. 8 and 9.

Table 1

THE WAVENUMBERS FOR A $TE_{z0\ell}$ MODE, OBTAINED BY (130), (133), and (98) OR (99)

ℓ	$\xi = 0.01$		$\xi = 0.01$, $w = 5$	
	$P = k_{x0}w$ (133)	$P = k_{x0}w$ (130)	k_z/k (130)	k_z/k (98) or (99)
0	3.027 - i.0314	3.030 - i.0294	.995 + i.907E - 4	.995 + i.874E - 4
1	6.082 - i.0628	6.086 - i.0593	.981 + i.372E - 3	.982 + i.359E - 3
2	9.147 - i.0942	9.153 - i.0894	.956 + i.867E - 3	.957 + i.835E - 3
3	12.220 - i.1257	12.226 - i.1197	.921 + i.161E - 2	.923 + i.155E - 2
4	15.297 - i.1571	15.303 - i.1500	.873 + i.266E - 2	.877 + i.256E - 2
5	18.378 - i.1885	18.385 - i.1804	.813 + i.413E - 2	.816 + i.397E - 2

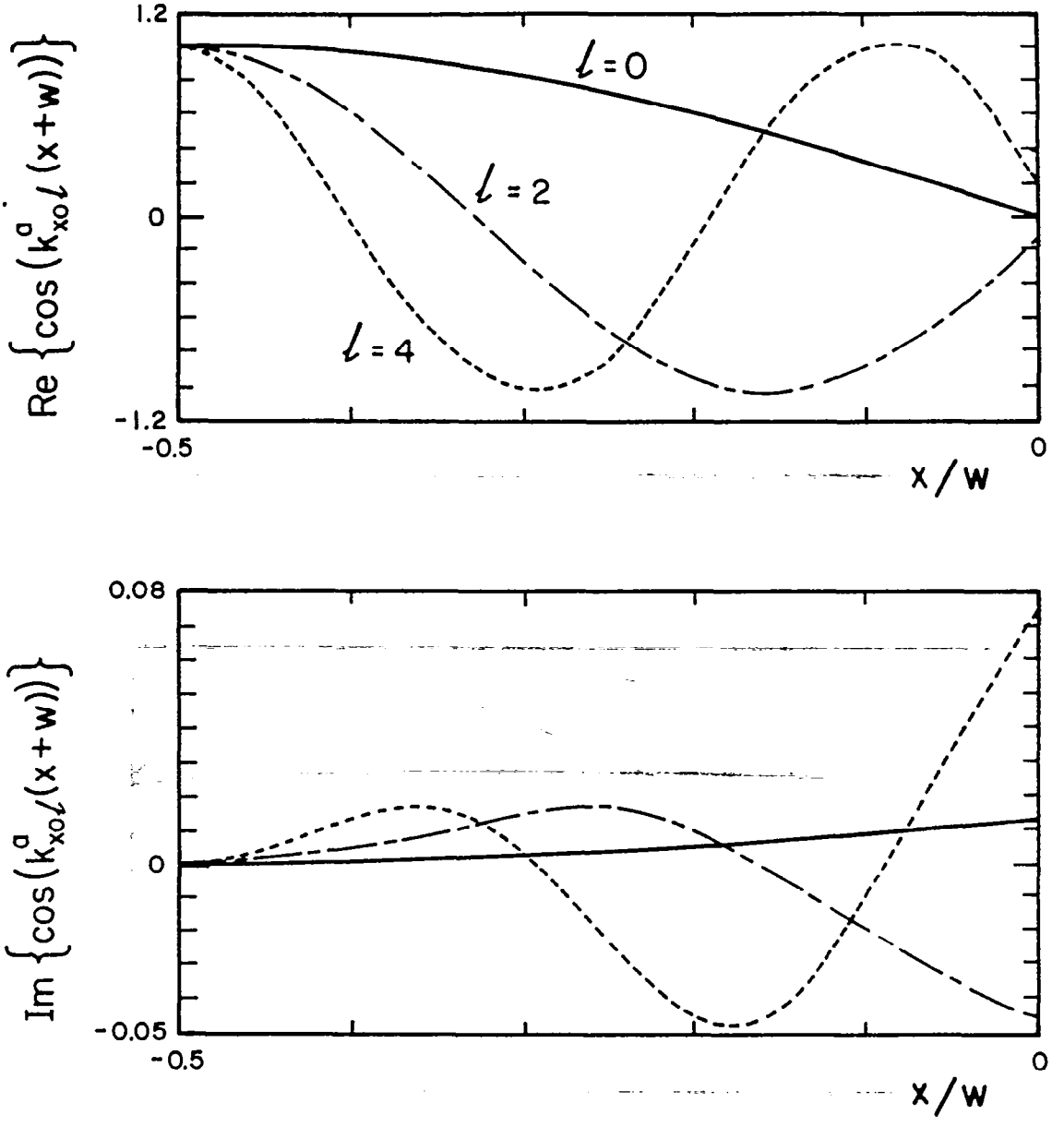

Figure 8a

The Normalized Longitudinal Magnetic Field of the Three Lowest Symmetric $TE_{z0\ell}$ Modes (ξ = 0.01).

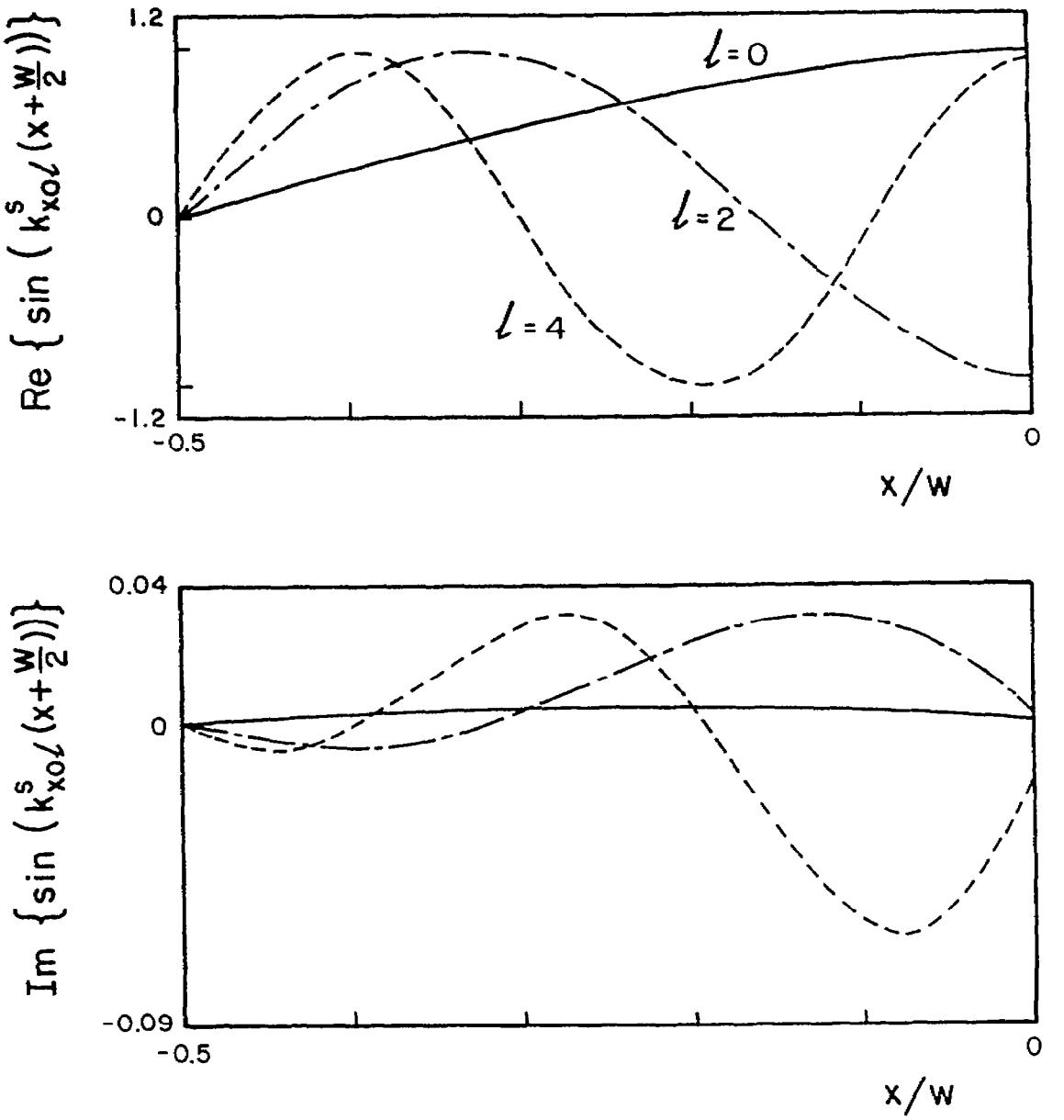

Figure 8b.

The Normalized Transverse Electric and Magnetic Fields of the Three Lowest Symmetric $TE_{z0\ell}$ Modes (ξ = 0.01).

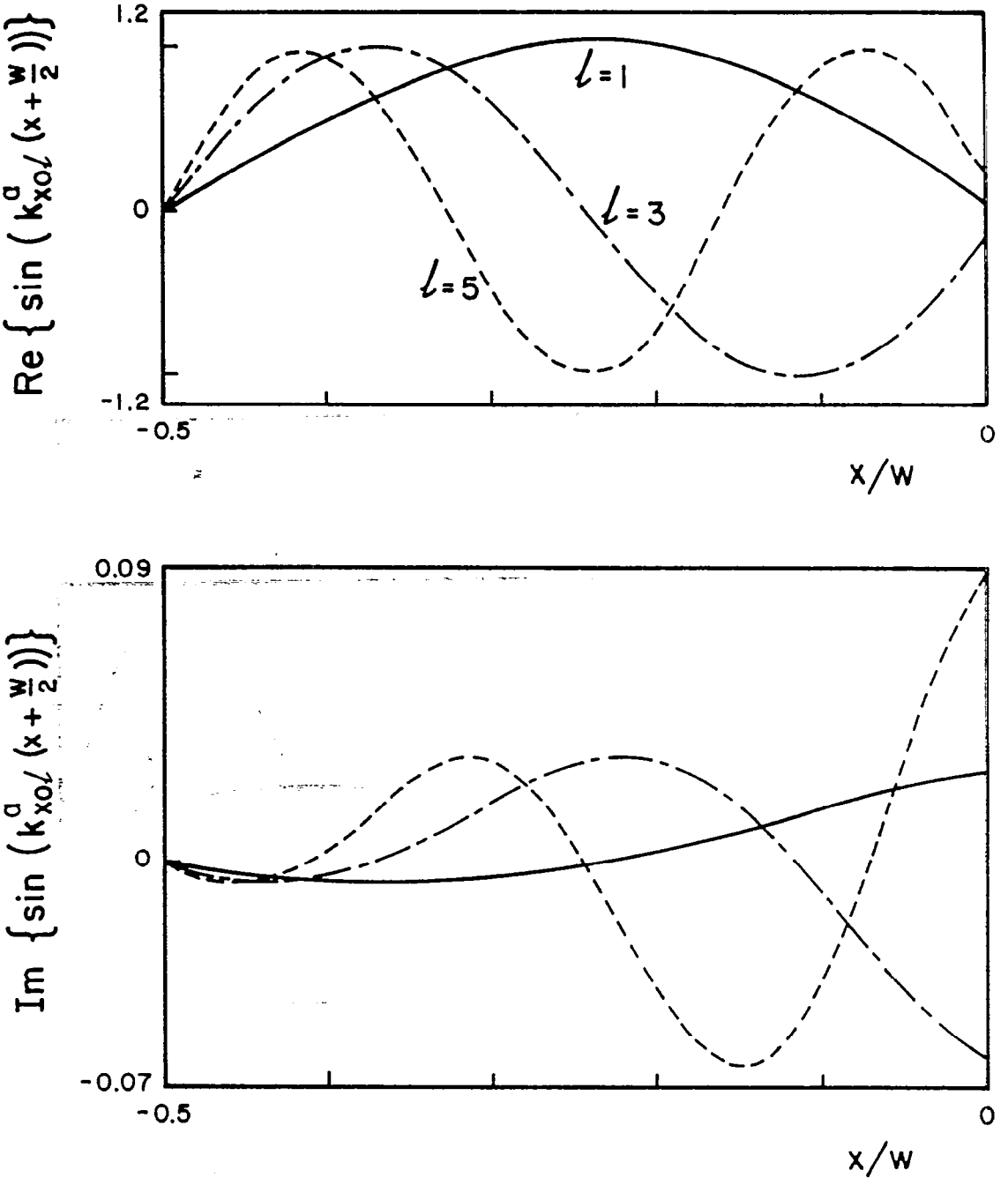

Figure 9a.

The Normalized Longitudinal Magnetic Field of the Three Lowest Antisymmetric $TE_{z0\ell}$ Modes (ξ = 0.01).

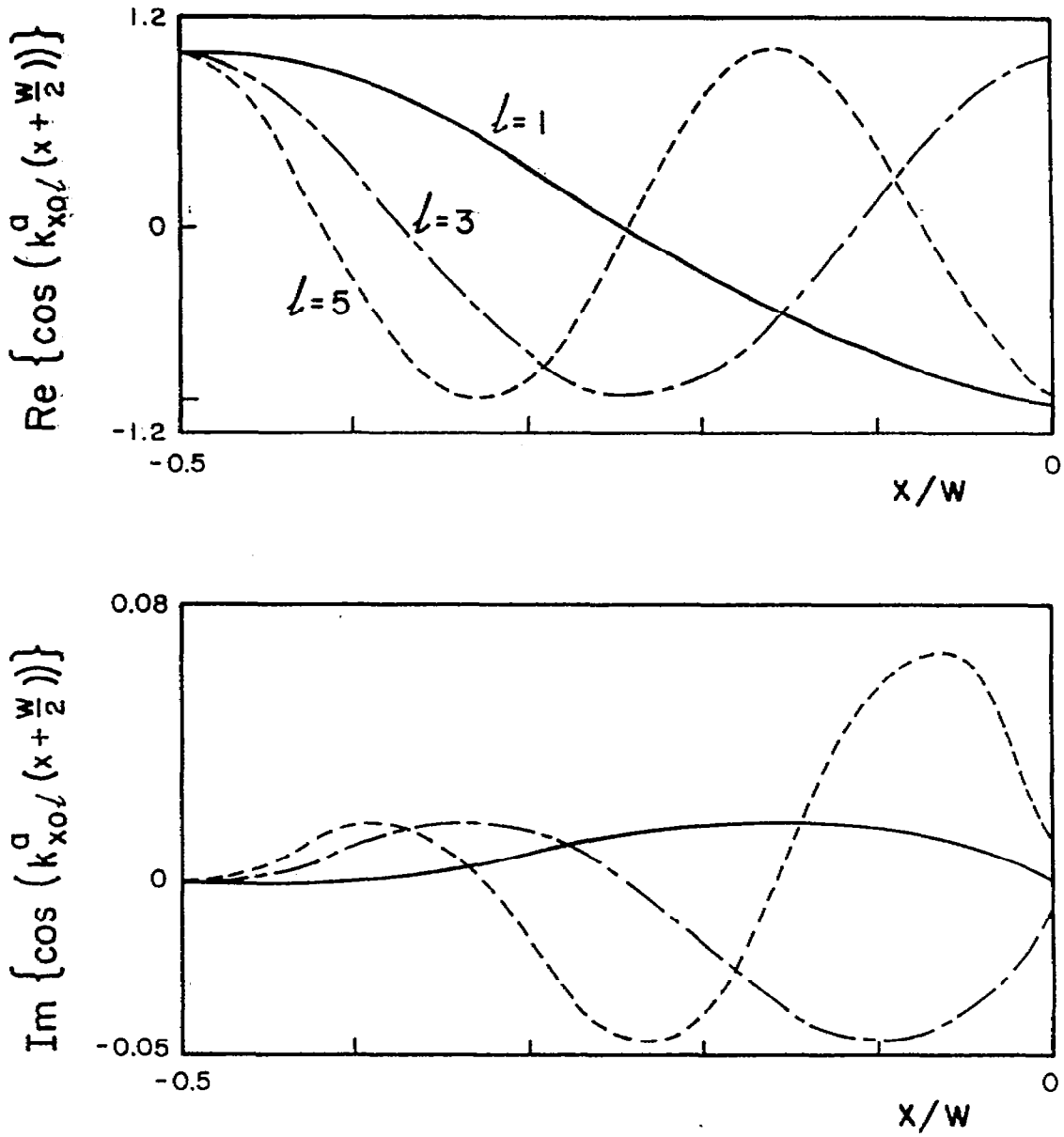

Figure 9b.

The Normalized Transverse Electric and Magnetic Fields of the Three Lowest Antisymmetric $TE_{z0\ell}$ Modes ($\xi_r = 0.01$).

APPENDIX A

THE SQUARE ROOT FUNCTION FOR k_x

For a leaky mode with $k_y = \frac{m\pi}{2h}$, the wavenumber $k_x = \beta_x + i\alpha_x$ (usually denoted k_{xm}) is obtained from the square root function

$$k_x = k_x(k_z) = \sqrt{k^2 - \left(\frac{m\pi}{2h}\right)^2 - k_z^2} = \sqrt{k_m^2 - k_z^2} \tag{A.1}$$

where

$$k_m = \sqrt{k^2 - \left(\frac{m\pi}{2h}\right)^2} \tag{A.2}$$

The transverse wavenumber k_t is a special case of (A.1) with m set equal to zero. Let

$$k_x^2 = |k_x|^2 \, e^{i\phi} \tag{A.3}$$

whence

$$k_x = |k_x| \, e^{i\frac{\phi}{2}} \tag{A.4}$$

It is evident from (A.3) that $k_x(k_z)$ will not be uniquely defined unless $\arg(k_x^2) = \phi$ is specified. To obtain a one-to-one correspondence between the k_x and k_x^2 planes, a two-sheeted k_x^2 plane is defined. This definition can be done in various ways. These are

$$\begin{aligned} \phi_0 \leq \phi < 2\pi + \phi_0 \quad &\text{(top sheet)} \\ 2\pi + \phi_0 \leq \phi < 4\pi + \phi_0 \quad &\text{(bottom sheet)} \end{aligned} \tag{A.5}$$

where ϕ_0 is arbitrary.

These Riemann sheets have their branch cut in the k_x^2 plane along the straight line $\phi = \phi_0$ or $\phi = 2\pi + \phi_0$. With the particular choice $\phi_0 = 0$, the entire top, or proper, sheet of the k_x^2 plane is characterized by

$\alpha_x = \text{Im}\, k_x > 0$ and the bottom, or improper, sheet by $\alpha_x < 0$. For a given value of k_x^2 one has the relation

$$\sqrt{k_x^2}\Big]_{\text{bottom}} = -\sqrt{k_x^2}\Big]_{\text{top}} \tag{A.6}$$

The two-sheeted k_x^2 plane maps into a two-sheeted k_z^2 plane, which in turn maps into a two-sheeted k_z plane. This last mapping is shown in Fig. 10.

Since k_z is restricted to the first quadrant (1), k_x can be only in the fourth quadrant (improper sheet) or in the second quadrant (proper sheet). In fact, if we define the real parameters C_1 and C_2

$$C_1 = \beta_x^2 - \alpha_x^2 = k^2 - \left(\frac{m\pi}{2h}\right)^2 - \beta_z^2 + \alpha_z^2 \tag{A.7}$$

$$C_2 = \beta_z \alpha_z = -\beta_x \alpha_x \tag{A.8}$$

then we have

$$\beta_x^4 - C_1 \beta_x^2 - C_2^2 = 0 \tag{A.9}$$

which gives

$$\beta_x = \pm\left[\frac{1}{2}\left(C_1 + \sqrt{C_1^2 + 4C_2^2}\right)\right]^{1/2} \tag{A.10}$$

and

$$\alpha_x = -\frac{C_2}{\beta_x} \tag{A.11}$$

The plus and minus signs in (A.11) correspond to the improper and proper sheets, respectively.

For a given k_z, if m in (A.7) is large enough, then C_1 is negative and $|C_1| >> C_2$. In this case (A.9) has the solutions $\beta_x^2 = C_1$ and

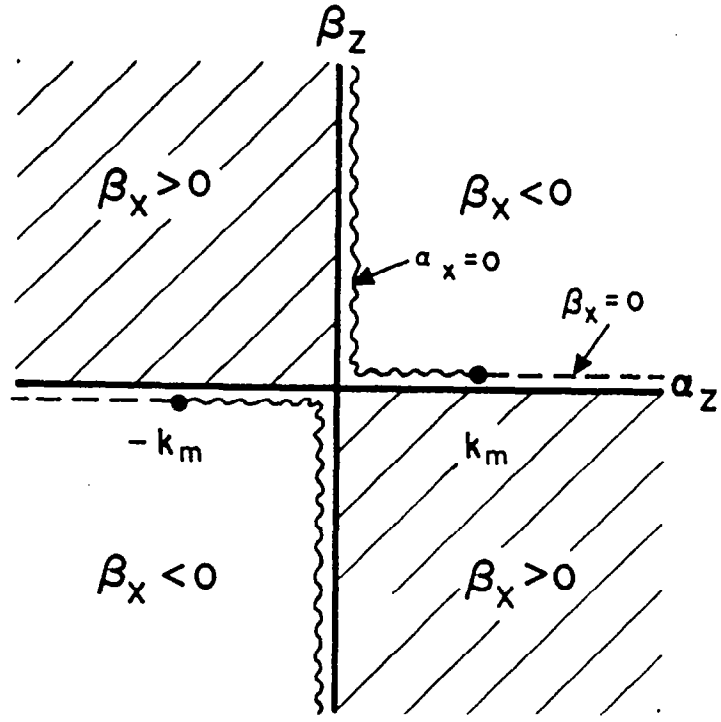

a. Top (proper) sheet $\alpha_x > 0$

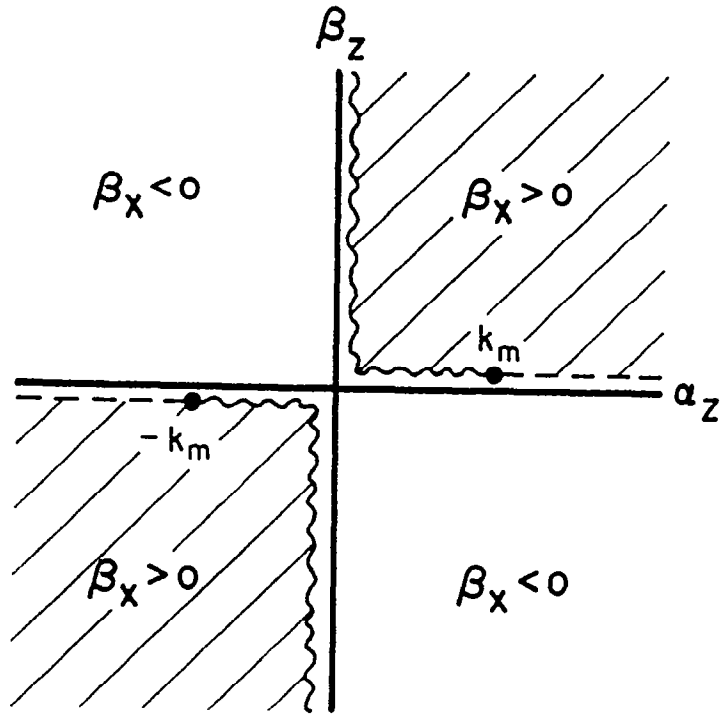

b. Bottom (improper) sheet $\alpha_x < 0$

Figure 10. Branch Cuts for $k_x(k_z)$.

branch cut $\alpha_x = 0$

$\beta_x = 0$

$\beta_x^2 = \left(-C_2^2/C_1\right)$, the second of which gives

$$\beta_x = \pm C_2/\sqrt{-C_1} \tag{A.12}$$

whence

$$\alpha_x = \mp\sqrt{-C_1} \tag{A.13}$$

Throughout this work, the value of k_x is meant to be that of the improper sheet.

APPENDIX B

FACTORIZATION FUNCTIONS G_+ and L_+

The reflection coefficient R_{nm} in equation (94) is expressed for even m,n in terms of $G_+(k_{xn})G_+(k_{xm})$. The G_+ function is given in equation (11.12d) of (ref. 8), and is repeated below

$$G_+(\eta) = G_-(-\eta) = \left(\frac{\sin k_t h}{k_t h}\right)^{1/2} B^e(\eta)C(\eta)P^e_\infty(\eta) \tag{B.1}$$

where

$$B^e(\eta) = \exp\left\{\frac{i\eta h}{\pi}\left[\ell n\left(\frac{2\pi}{k_t h}\right) + (1 - C) + i\,\frac{\pi}{2}\right]\right\} \tag{B.2}$$

$$C(\eta) = \exp\left[\frac{i\gamma h}{\pi}\,\ell n\left(\frac{\eta - \gamma}{k_t}\right)\right] \tag{B.3}$$

and

$$P^e_\infty(\eta) = \prod_{\substack{n=2 \\ n\ \text{even}}}^{\infty}\left(1 + \frac{\eta}{\eta_n}\right)\exp\left(i\,\frac{2\eta h}{n\pi}\right) \tag{B.4}$$

As indicated in section V, we replace every k by k_t. γ in (B.3) is given by (9) and η_n in (B.4) is given by

$$\eta_n = \pm\sqrt{k_t^2 - \left(\frac{n\pi}{2h}\right)^2} = \pm k_{xn} \tag{B.5}$$

The G_+ function is defined in equation (B.1) in terms of some multivalued functions that need to be specified so that G_+ becomes uniquely defined.

Since the factor $\left(\frac{\sin k_t h}{k_t h}\right)$ rather than its square root appears in R_{nm}, it represents no ambiguity.

In $B^e(\eta)$, if we let $k_t = |k_t| \exp(i \arg k_t)$, then the infinitely multiple-valued logarithmic function

$$\ln\left(\frac{2\pi}{k_t h}\right) = \ln\left(\frac{2\pi}{|k_t|h}\right) - i(\arg k_t + 2\ell\pi) \tag{B.6}$$

is specified to have the unique value corresponding to $\ell = 0$. This choice is in agreement with the definition of the log function in the real limit of k_t, i.e., as $\arg k_t \to 0$.

In $C(k_{xm})$ we have

$$\gamma = -i\left(k_t^2 - k_{xm}^2\right)^{1/2} = -ik_{ym} \tag{B.7}$$

whence

$$C(k_{xm}) = \exp\left(\frac{m}{2}\left\{\ln\left|\frac{k_{xm} + ik_{ym}}{k_t}\right| + i\left[\arg\left(k_{xm} + ik_{ym}\right) - \arg k_t\right]\right\}\right) \tag{B.8}$$

where

$$\arg\left(k_{xm} + ik_{ym}\right) = \begin{cases} \tan^{-1}\left(\dfrac{\alpha_{xm} + k_{ym}}{\beta_{xm}}\right) & \text{for } \alpha_{xm} + k_{ym} > 0 \\ -\tan^{-1}\left[\dfrac{-\left(\alpha_{xm} + k_{ym}\right)}{\beta_{xm}}\right] & \text{for } \alpha_{xm} + k_{ym} \leq 0 \end{cases} \tag{B.9}$$

This specification of $C(k_{xm})$ is in agreement with its definition for $\alpha_{xm} = 0$ and ensures its continuity as $(\alpha_{xm} + k_{ym})$ changes.

In $P_\infty^e(k_{xm})$ it was observed that, for large n

$$\eta_n = -k_{xn} \simeq i\,\frac{n\pi}{2h} \qquad n \text{ large} \tag{B.10}$$

For small n (at least for $n \leq m$)

$$\eta_n = +k_{xn} \qquad n \text{ small} \tag{B.11}$$

The transition of η_n from $+k_{xn}$ to $-k_{xn}$ is determined according to the criterion

$$\eta_n = \begin{cases} +k_{xn} & \text{if Re } \left(k_t^2\right) > \left(\frac{n\pi}{2h}\right)^2 \\ -k_{xn} & \text{if Re } \left(k_t^2\right) < \left(\frac{n\pi}{2h}\right)^2 \end{cases} \tag{B.12}$$

This criterion is analogous to that used in a two-dimensional problem where k_t is real.

If m and n are odd, then R_{nm} in equation (94) is expressed in terms of $L_+(k_{xn})L_+(k_{xn})$, with the L_+ function given by

$$L_+(\eta) = L_-(-\eta) = (\cos k_t h)^{1/2} B^0(\eta) C(\eta) P_\infty^0(\eta) \tag{B.13}$$

where

$$B^0(\eta) = \exp\left\{\frac{i\eta h}{\pi}\left[\ell n\left(\frac{\pi}{2k_t h}\right) + (1 - C) + i\,\frac{\pi}{2}\right]\right\} \tag{B.14}$$

and

$$P_\infty^0(\eta) = \prod_{\substack{n=1 \\ n \text{ odd}}}^{\infty} \left(1 + \frac{\eta}{\eta_n}\right) \exp\left(i\,\frac{2\eta h}{n\pi}\right) \tag{B.15}$$

APPENDIX C

TRUNCATION OF THE INFINITE PRODUCT

To evaluate the G_+ function, we need to evaluate the infinite product needs to be evaluated.

$$P_\infty^e(\eta) = \prod_{\substack{m=2 \\ m \text{ even}}}^{\infty} \left(1 + \frac{\eta}{\eta_m}\right) \exp\left(i \frac{2\eta h}{n\pi}\right)$$

$$= \prod_{m=1}^{\infty} \left(1 + \frac{\eta}{t_m}\right) \exp\left(\frac{i\eta h}{m\pi}\right) \qquad (C.1)$$

where

$$t_m = \pm\sqrt{k_t^2 - \left(\frac{m\pi}{h}\right)^2} \xrightarrow[m \text{ large}]{} i\,\frac{m\pi}{h} \qquad (C.2)$$

In actual computation, this product is truncated to

$$P_M^e(\eta) = \prod_{m=1}^{M} \left(1 + \frac{\eta}{t_m}\right) \exp\left(\frac{i\eta h}{m\pi}\right) \qquad (C.3)$$

The relative error introduced due to this truncation is

$$\varepsilon_M(\eta) = \left|\frac{P_\infty^e(\eta) - P_M^e(\eta)}{P_M^e(\eta)}\right|$$

$$= \left|\prod_{m=M+1}^{\infty} \left(1 + \frac{\eta}{t_m}\right) e^{i\,\frac{\eta h}{m\pi}} - 1\right| \qquad (C.4)$$

For large m

$$\left(1 + \frac{\eta}{t_m}\right) e^{i\frac{\eta h}{m\pi}} \approx \left(1 - i\frac{\eta h}{m\pi}\right)\left[1 + i\frac{\eta h}{m\pi} - \frac{1}{2}\left(\frac{\eta h}{m\pi}\right)^2 + \ldots\right]$$

$$\approx \left[1 + \frac{1}{2}\left(\frac{\eta h}{m\pi}\right)^2 + \ldots\right] \qquad (C.5)$$

by neglecting terms whose order is smaller than $\left(\frac{\eta h}{m\pi}\right)^2$

$$\therefore \varepsilon_M(\eta) \approx \left| \prod_{m=M+1}^{\infty} \left[1 + \frac{1}{2}\left(\frac{\eta h}{m\pi}\right)^2\right] - 1 \right|$$

$$\approx \frac{1}{2}\left|\frac{\eta h}{\pi}\right|^2 \sum_{m=M+1}^{\infty} \frac{1}{m^2} \qquad (C.6)$$

but

$$\sum_{m=M+1}^{\infty} \frac{1}{m^2} < \int_M^{\infty} \frac{dx}{x^2} = \frac{1}{M} \qquad (C.7)$$

Therefore,

$$\varepsilon_M(\eta) \approx \frac{1}{2M}\left|\frac{\eta h}{\pi}\right|^2 \qquad (C.8)$$

If $\varepsilon_M(\eta)$ is specified to be less than some number $\varepsilon_{max} << 1$, then

$$M > \frac{1}{2}\left|\frac{\eta h}{\pi}\right|^2 \frac{1}{\varepsilon_{max}} \qquad (C.9)$$

This requires that $|\eta h|$ be not too large; otherwise the convergence of $P_\infty^e(\eta)$ becomes prohibitively slow.

For $\varepsilon_{max} \approx \frac{1}{2} \times 10^{-4}$ we took

$$M_{min} = 10^3\left(\eta_1^2 + \eta_2^2\right) h^2 \qquad (C.10)$$

where η_1, η_2 are the real and imaginary parts of η, respectively.

A similar truncation is used for $P_\infty^0(\eta)$ while evaluating the L_+ function.

REFERENCES

1. Baum, C. E., "Impedance and Field Distributions for Parallel Plate Transmission Line Simulators," Sensor and Simulation Note 21, June 1966.

2. Baum, C. E., "General Principles for the Design of ATLAS I and II, Part V: Some Approximate Figures of Merit for Comparing the Waveforms Launched by Imperfect Pulser Arrays onto TEM Transmission Lines," Sensor and Simulation Note 148, May 1972.

3. Brown, T. L., and Granzow, K. D., "A Parameter Study of Two-Parallel-Plate Transmission Line Simulators of EMP Sensor and Simulation Note 21," Sensor and Simulation Note 52, April 1968.

4. Baum, C. E., Giri, D. V., and Gonzalez, R. D., "Electromagnetic Field Distribution of the TEM Mode in a Symmetrical Two-Parallel-Plate Transmission Line," Sensor and Simulation Note 219, April 1976.

5. Marcuvitz, N., "On Field Representation in Terms of Leaky Modes or Eigenmodes," IRE Trans. Antennas Propagat., AP-4, pp. 192-194, 1956.

6. Hessel, A., "General Characteristics of Travelling-Wave Antennas," Chapter 19 in Antenna Theory, eds., R. E. Collin and F. J. Zucker, McGraw-Hill, New York, 1969.

7. Marin, L., "Modes on a Finite-Width, Parallel-Plate Simulator. I. Narrow Plates," Sensor and Simulation Note 201, September 1974.

8. Mittra, R., and Lee, S. W., Analytical Techniques in the Theory of Guided Waves, Macmillan, New York, 1971.

9. Collin, R. E., Foundations for Microwave Engineering, McGraw-Hill, New York, 1966.

10. Lee, S. W., "Ray Theory of Diffraction by Open-Ended Waveguides. II. Applications," J. Math. Phys., 13, 5, May 1972.

11. Lee, S. W., and Deschamps, G. A., "A Uniform Asymptotic Theory of Electromagnetic Diffraction by a Curved Wedge," Electromagnetics Laboratory Scientific Report No. 74-18, University of Illinois at Urbana-Champaign, Urbana, Illinois, December 1974.

12. Muller, D. E., "A Method for Solving Algebraic Equations Using an Automatic Computer," Mathematical Tables and Other Aids to Computation, 56, October 1956.

13. Singaraju, K., Giri, D., and Baum, C., "Further Developments in the Application of Contour Integration to the Evaluation of the Zeros of Analytic Functions and Relevant Computer Programs," Mathematics Note 42, March 1976.

14. Marin. L., "Modes on a Finite-Width, Parallel-Plate Simulator, Part II. Wide Plates," Sensor and Simulation Note 223, March 1977, revised November 1977.

15. Boersma, J., "Analysis of Weinstein's Diffraction Function," Philips Res. Repts., 30, pp. 161-170, 1975 (Issue in honor of C. J. Bouwkamp).

16. Weinstein, L. A., The Theory of Diffraction and the Factorization Method, The Golem Press, Boulder, Colorado, 1969.

Weinstein, L. A., Open Resonators and Open Waveguides, The Golem Press, Boulder, Colorado, 1969.

17. Krichevsky, V. and Mittra, R., "Source Excitation of an Open Parallel-Plate Waveguide," Electromagnetics Laboratory, Report No. 77-19, University of Illinois at Urbana-Champaign, Urbana, Illinois, September 1977.